UFS

UNIVERSITY OF THE FREE STATE
UNIVERSITEIT VAN DIE VRYSTAAT
YUNIVESITHI YA FREISTATA

Dual *in-vitro* effects of *cannabis* on inflammatory bio-markers in triple-negative breast cancer and arthritis

DOREEN KULABAKO KYAGABA (Student No.: 2015046101)

Submitted in fulfilment of the requirements in respect of the Master's Degree MMedSc in the Department of Pharmacology in the Faculty of Health Sciences at the University of the Free State (UFS).

Submission date: 2 December 2024

Supervisor: Prof Mamello P. Sekhoacha (UFS)

Co-Supervisors: Dr. Victoria Fasiku (UFS) and Prof David Katerere of Tshwane University of Technology (TUT)

Declaration of authorship

I, Doreen Kulabako Kyagaba declare that the Master's Degree research dissertation that I herewith submit for the Master's Degree qualification Pharmacology at the University of the Free State is my independent work, and that I have not previously submitted it for a qualification at another institution of higher education.

Signature:

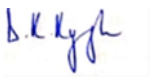

Acknowledgments

To everyone who contributed to the successful completion of my Master's dissertation, I would like to extend my sincere gratitude. It has been a challenging but worthwhile journey, and I am sincerely grateful for all the support and encouragement I received throughout:

- My devoted parents, Mr. Peter Kyagaba and Mrs. Rethabile Kyagaba, for their unwavering belief in me, prayers, support, and encouragement even during the most trying times.
- Prof. Mamello Sekhoacha (UFS, Pharmacology), my supervisor, for her outstanding leadership and guidance throughout this process.
- Dr. Victoria Fasiku (UFS, Pharmacology), my co-supervisor, for the invaluable assistance with cell culture experiments, for the dedication and for always being available for consultation on critical research matters.
- Prof. David Katerere (TUT, Pharmaceutical Sciences), my co-supervisor, for his guidance on *Cannabis sativa* processing experiments and providing access to required equipment and materials. For facilitating key connections with colleagues and industry experts (Dr. Illiassou Mouafon, Dr. Manikandan Gurusamy, Mr. Pollen Nkuna and Miss Olwethu Mtombeni) who were also ever-willing to assist.
- Dr. Gabre Kemp (Biochemistry, UFS) for kindly lending his knowledge and providing access to facilities for Liquid Chromatography-Mass Spectrometry (LC-MS) experiments.
- Dr. Beynon Abrahams, Dr. Claudia Ntsapi (Biomedical Sciences, UFS) and Miss Viwe Fokazi for their assistance with access to laboratory equipment and material required for different *in-vitro* experiments.
- Dr. Claudia Ntsapi for giving training on the Western blot protocol, and Miss Nandi Mabaso for sharing her previous Masters research work experience and practical knowledge of the technique.
- Above all, I thank God almighty for this opportunity to learn and grow and, for giving me the strength and resilience to persevere.

To each of you, I extend my heartfelt thanks for your contributions, which have been crucial to making this work a reality.

Research Outputs

- Drafted a review article provisionally entitled "Mechanisms of *Cannabis sativa* in the Treatment of Breast Cancer and Arthritis." The article examines the prevalent mechanisms by which *C. sativa* mitigates breast cancer and arthritis. It is presently under internal review, with publication planned for 2025.
- Successfully submitted a Master's dissertation in a record timeframe. The research findings will form the basis of a second article, tentatively titled "Investigating the Impact of *Cannabis sativa* on Key Proteins Related to Breast Cancer and Arthritis."
- Acquired advanced technical skills and knowledge, including proficiency in LC-MS, cell culture, Western blotting, and Enzyme-Linked Immunosorbent Assay (ELISA) techniques, important for conducting innovative biomedical research.
- Engaged in interdisciplinary collaboration by working with specialists in pharmaceutical sciences, basic medical sciences, and biochemistry, thereby promoting a holistic approach to *C. sativa*-related pharmacology research.
- Reported preliminary research findings during weekly departmental presentations and an institutional three-minute thesis competition, obtaining constructive feedback to enhance methodologies and interpretations.

Table of Figures

List of Tables

List of Abbreviations

(L.)	Linnaeus
2-AG	2-arachidonoyl glycerol
5-HT	serotonin
5-LO	5-lipoxygenase
α	alpha
β-ME	β-Mercaptoethanol
γ	Gamma
AE	Anandamide or N-arachidonoyl ethanolamine
AjA	Ajulemic acid
ANOVA	Analysis of Variance
AP	Alkaline phosphatase
AUC	Area under the curve
BCA	Bicinchoninic acid
BSA	Bovine serum albumin
BL	Basal
CBC	Cannabichromene
CBD	Cannabidiol
CBDA	Cannabidiolic acid
CBDV	Cannabidivarin
CBG	Cannabigerol
CBGA	Cannabigerolic acid
CBGV	Cannabigerovarin
CBN	Cannabinol
CBR	Cannabinoid receptor
CIA	Collagen-induced arthritis
CNIV	Chemotherapy-induced nausea and vomiting
CO_2	Carbon dioxide
COA	Certificate of Analysis
COX	Cyclooxygenase
CSIR	Council for Scientific and Industrial Research
dH_2O	Distilled water
DMARDs	Disease-modifying antirheumatic drugs

DMEM	Dulbecco's modified eagle medium
DMSO	Dimethyl sulfoxide
DOX	Doxorubicin
E+H	Ethanol and water (1:1)
EBREC	Environmental Biosafety Research Ethics Committee
ECL	Enhanced Chemiluminescence
ECM	Extracellular matrix
ECS	Endocannabinoid system
EGF	Epidermal growth factor
EGFR	Epidermal growth factor receptor
ELISA	Enzyme-Linked immunosorbent assay
EMA	European Medicines Agency
ER	Estrogen receptor
ER stress	Endoplasmic reticulum stress
ERK	Extracellular signal-regulated kinase
FAK	Focal adhesion kinase
FBS	Foetal bovine serum
FDA	Federal Drug Administration
FECO	Full Extract Cannabis Oil
FLS	Fibroblast-like synovial cells
GC-FID	Gas chromatography with flame ionization detection
GPR or GPCR	G protein-coupled receptor
HER	Human epidermal growth factor receptor
HIV/AIDS	Human immunodeficiency virus/Acquired immunodeficiency syndrome
HOX	homeobox genes
HPLC	High Performance Liquid Chromatography
HRP	Horse radish peroxidase
IFN	Interferon
IL	Interleukin
IM	Immunomodulatory
iNOS	inducible nitric oxide synthase
kD	Kilodaltons

LAR	Luminal androgen-receptor
LC-MS	Liquid Chromatography Mass Spectrometry
LPS	Lipopolysaccharide
M	Mesenchymal
MAPK	Mitogen-activated protein kinase
MMP	Matrix metalloproteinase
MSL	Mesenchymal stem-like
mTOR	Mammalian target of rapamycin
MTT	3-[4,5-dimethylthiazol-2-yl]-2,5 diphenyl tetrazolium bromide
MTX	Methotrexate
NAFS	National Analytical Forensic Services
$NaNO_2$	Sodium nitrite
NCI	National Cancer Institute
NF-kB	Nuclear factor kappa B
NSAIDs	Non-steroidal anti-inflammatory drugs
NSB	Non-specific binding
PI3K	Phosphatidylinositol 3-kinases
PBS	Phosphate buffered saline
PGE	Prostaglandin E
PMBC	Peripheral mononuclear blood cells
PPAR	Peroxisome proliferator-activated receptor
PR	Progesterone receptor
Prof.	Professor
RA	Rheumatoid arthritis
RANK-L	Receptor activator of nuclear factor KB ligand
RASF	Rheumatoid arthritis synovial fibroblasts
RF	Rheumatoid factor
Rho	Ras homolog
RIPA	Radioimmunoprecipitation assay
ROS	Reactive oxygen species
RT	Retention time
SCF	Supercritical fluid carbon dioxide
SD	Standard deviation

SDS	Sodium dodecyl sulfate
TA	Total activity
TAM	Tumour Associated Macrophages
THC	Tetrahydrocannabinol
THCA	Tetrahydrocannabinolic acid
THCV	Tetrahydrocannabivarin
THCVA	Tetrahydrocannabivarinic Acid
TIC	Total ion chromatogram
TNBC	Triple-negative breast cancer
TNF	Tumor Necrosis Factor
TRPV	Transient receptor potential vanilloid
TUT	Tshwane University of Technology
UFS	University of the Free State
USA	United States of America
XIC	Extracted-ion chromatogram

Table of Contents

ABSTRACT

Context: Triple-negative breast cancer (TNBC) is an aggressive subtype of breast cancer with the poorest treatment outcomes, while rheumatoid arthritis (RA) is a debilitating disorder in which joints and surrounding tissue undergo degradation due to autoimmunity. Chronic inflammation underpins the pathophysiology of both these conditions. *Cannabis sativa* (L) has gained popularity beyond its recreational use, with scientific research highlighting anti-cancer and anti-inflammatory properties. However, extensive evidence is still needed to validate many of its medical applications, including use in breast cancer and arthritis. **Aim**: This research aimed to study the effects of *Cannabis sativa* extracts on TNBC and RA progression and the inflammatory biomarkers present in both conditions. **Methods**: Two types of *C. sativa*-derived products were investigated, i.e., the oil and spent-biomass obtained from Supercritical fluid carbon dioxide (SCF) extraction. The spent-biomass was subjected to further sequential solvent extraction using different solvents. The extracts were then analysed for cannabinoid content to understand subsequent bioassays which were conducted to assess cytotoxicity and the expression of key inflammatory biomarkers in different cell lines. **Results and Discussion**: The greatest yield was obtained from SCF extraction (17.3%). Although the total spent-biomass extract yield (18.2%) was slightly higher, individual extract yields were lower in comparison to SCF, however, they increased with increasing solvent polarity- hexane (1.65%), acetone (3.22%), methanol (5.78%) and ethanol and water (7.51%). Liquid Chromatography-Mass Spectrometry (LC-MS) revealed the presence of several cannabinoids (CBD, THC, THCA, CBDA, CBGA, CBC, CBG and, CBN). 3-(4,5-Dimethylthiazol-2-yl)-2,5-diphenyltetrazolium bromide (MTT) assay in MDA-MB-231, Vero and Lipopolysaccharide (LPS)-stimulated RAW 264.7 macrophages showed that SCF, hexane and acetone extracts were the most cytotoxic. Treatment of LPS-activated macrophages, which model inflammation in both TNBC and RA, with the most potent extracts (SCF and acetone) resulted in significant suppression of nitrites and Prostaglandin E_2 (PGE2). Potential downregulation of Cyclooxygenase-2 (COX-2), Interleukin-6 (IL-6) and Tumor Necrosis Factor-Alpha (TNF-α) was also observed qualitatively from Coomassie-blue staining. **Conclusion:** These findings suggest that *C. sativa's* diverse phytochemicals, particularly its unique cannabinoid-rich profile, largely contribute to its potent anticancer and anti-inflammatory effects. However,

future work is recommended to enhance specificity and dosage standardization to maximize efficacy and safety.

CHAPTER 1: INTRODUCTION

1.1 Background

The usefulness of *Cannabis sativa* (L.) has been recognised by mankind for several thousands of years, and recently it has gained popularity in medical research (Balant *et al.*, 2021). Historical applications of *C. sativa* include dietary consumption, religious rituals, making textiles and medicinal use (Balant *et al.*, 2021). More recently and relevant to the present study, a wider range of ethnopharmacological benefits have been identified, from various palliative treatments to anti-inflammatory, analgesic, and anti-cancer activity (Pellati *et al.*, 2018). These medicinal properties are attributed to *C. sativa's* phytochemical-rich profile, with emphasis being placed on cannabinoids in most studies (Aizpurua-Olaizola *et al.*, 2014; Farinon *et al.*, 2020; Lal *et al.*, 2021; Legare, Raup-Konsavage and Vrana, 2022).

Chronic inflammation is a persistent immune response that plays a significant role in various diseases, including breast cancer and arthritis (Pol *et al.*, 2022). In breast cancer, chronic inflammation drives tumour cell proliferation and metastasis through an inflammatory tumour microenvironment rich in immune cells, such as tumour-associated macrophages, and reactive oxygen species (ROS) production, which cause cell damage and promote tumorigenicity (Danforth, 2021; Villarreal-García *et al.*, 2022). In arthritis, chronic inflammation leads to joint damage, driven by several inflammatory mediators such as cytokines (Mariani *et al.*, 2023; Sarzi-Puttini *et al.*, 2024).

Breast cancer and arthritis are statistically among the most prevalent disorders globally and in South Africa (Usenbo *et al.*, 2015; Blasco-Benito *et al.*, 2018). These two diseases can be studied together as they share commonalities in terms of their initiation and pathophysiological processes, which present opportunities for discovering a dual-targeting treatment approach for both diseases.

There are significant similarities between cancer and rheumatoid arthritis. First, rheumatoid arthritis is also a non-communicable disorder that involves an immune-mediated inflammatory response and is sustained by an inflammatory microenvironment (McInnes and Schett, 2017). Second, similarly to breast cancer,

rheumatoid arthritis disproportionately affects more women than men (Poudel, Goyal and Lappin, 2022). Third, similarly to the abnormally rapid cell proliferation and mutation seen in cancerous cells, synovial fibroblasts undergo hyperplasia in inflammatory arthritis such as rheumatoid arthritis (Poudel, Goyal and Lappin, 2022).

Rheumatoid arthritis

Rheumatoid arthritis is the most prevalent type of autoimmune inflammatory arthritis (Chang and Nigrovic, 2019). Up to 54% of patients with undifferentiated inflammatory arthritis are predicted to develop rheumatoid arthritis. It is commonly seen in upper and lower extremity joints and the distal interphalangeal joints of the hands, and it frequently presents with aggressive synovitis (Chang and Nigrovic, 2019; Poudel, Goyal and Lappin, 2022). More general symptoms include common signs of inflammation, such as pain, swelling, and tenderness in the joints, accompanied by a heat sensation and morning stiffness. These symptoms result from cartilage degradation and synovium inflammation (Poudel, Goyal and Lappin, 2022). The long-term clinical manifestations of untreated rheumatoid arthritis include ulnar drift, swan neck deformity, and subcutaneous nodules (Dudics *et al.*, 2018).

Presently, standard treatments for inflammatory arthritis, such as in the case of rheumatoid arthritis, are based on managing the symptoms as there is no cure. Common rheumatoid arthritis medications are categorised into non-steroidal anti-inflammatory drugs (NSAIDs) and biologic and chemical disease-modifying antirheumatic drugs (DMARDs). Biologic DMARDs are costly, they are associated with severe adverse effects, and they provide therapy that is only beneficial to a fraction of patients (Dudics *et al.*, 2018).

Breast cancer

Breast cancer is a leading cause of malignancy among women worldwide, with 2.3 million confirmed cases and 670 000 deaths recorded in 2022 (Yin *et al.*, 2020; WHO, 2024). Despite efforts such as early diagnosis and improved therapy to reduce mortality rates, treatment efficacy is limited by a lack of specificity, resistance and adverse side effects (Yin *et al.*, 2020).

The treatment for breast cancer includes surgery, radiation and systemic therapy (endocrine therapy, antibody therapy and chemotherapy) (Waks and Winer, 2019).

However, effectively treating breast cancer is a challenge due to its diverse characteristics. There are multiple subtypes, each one with a variable response to the different treatment options, and this leads to poorer prognoses and a high susceptibility to relapse (Sukumar *et al.*, 2021). Highly invasive triple-negative breast cancer is the most aggressive subtype of breast cancer (Sukumar *et al.*, 2021). Unlike other subtypes consisting of known bio-markers that allow for target-specific treatment, triple-negative breast cancer-unique bio-markers are still under investigation and present an opportunity for finding effective treatments (Sukumar *et al.*, 2021). Triple-negative breast cancer is not sensitive to standard endocrine and Human Epidermal Growth Factor Receptor 2 (HER2) breast cancer therapy treatments due to the absence or under-expression of established breast cancer bio-markers such as Estrogen Receptor (ER), Progesterone Receptor (PR) and HER2 receptors. Instead, patients rely on systemically strenuous chemotherapy treatments that are non-selectively cytotoxic and cause extreme negative side effects such as peripheral neuropathy, myelosuppression, cardiotoxicity, nephrotoxicity and gastrointestinal issues (Yin *et al.*, 2020)). Therefore, standardized target-specific triple-negative breast cancer regimens are an urgent clinical need.

Common modulators

Underlying the pathogenesis of triple-negative breast cancer and rheumatoid arthritis are common components of chronic inflammation and hyper-plasticity. These commonalities allow for the possibility of discovering dual-targeting treatment approaches for both conditions (Singh *et al.*, 2019). Novel approaches to developing more targeted treatments that can treat both conditions simultaneously could include targeting the immune cell microenvironment via receptor modulation or regulating common Nuclear Factor Kappa-Light-Chain-Enhancer of Activated B Cells (NF-kB) and Mitogen-Activated Protein Kinase (MAPK) inflammatory signalling pathway downstream bio-markers such as Cyclooxygenase-2 (COX-2), Interleukin-6 (IL-6) and Tumor Necrosis Factor-Alpha (TNF-α) (McInnes and Schett, 2017). *C. sativa* has been reported to have *in-vitro* anti-inflammation and antineoplastic action (Nagarkatti *et al.*, 2009; Kisková *et al.*, 2019) making it a good candidate to research.

Thus, the focus of this study will be on the use of *C. sativa* in triple-negative breast cancer and inflammatory arthritis, in particular rheumatoid arthritis.

1.2 Problem statement

An estimated 1.7 million females are diagnosed with breast cancer globally, and it accounts for 60% of deaths in developing countries each year (da Costa Vieira *et al.*, 2017). Triple-negative breast cancer has the shortest survival time with a mortality rate of ~40% within five years of detection, which rises to 75% three months after recurrence. It also has a metastasis incidence rate of 46%, often occurring in the brain and visceral organs (Yin *et al.*, 2020). Treatment options are not tumour-specific and are accompanied by serious adverse effects, which can lead to some patients opting out of therapy (Yin *et al.*, 2020).

On the other hand, rheumatoid arthritis affects one to two percent of people globally, but it has a collectively substantial negative impact due to its debilitating effects, including severe disability, significantly reduced quality of life and productivity, and the associated high medical costs (Chang and Nigrovic, 2019). The mode of action of current rheumatoid arthritis standard drugs is insufficient to completely cure the disease; they only relieve some associated symptoms such as pain and inflammation. Furthermore, there is a concerning rate of treatment failure; hence, more studies to find new therapeutic agents for these conditions are required.

1.3 Justification

Chronic inflammation is a key driver of cancer and arthritis. In cancer, extrinsic and intrinsic mechanisms are responsible for tumorigenesis and accelerating tumour progression, respectively (Singh *et al.*, 2019). In both conditions, the inflammatory microenvironment consisting of immune cells, host stromal cells, cancer or synovial fibroblast cells, plays a crucial role in initiating and sustaining the disease state (Singh *et al.*, 2019). As several intracellular signalling pathways, such as the activation of protein kinases and transcription factors, are dysregulated, the downstream effect is the aberrant expression of proinflammatory genes and therefore the excessive expression, synthesis and uncontrolled activation of inflammatory mediators such as COX-2, PGE2, and cytokines (IL-6, TNF-α) (Kundu and Surh, 2012). Together these promote cancer cells or synovial fibroblast hyperplasia, invasion and angiogenesis, while further perpetuating chronic inflammation in a vicious, deadly cycle.

Reports link breast cancer to aberrant stimulation of cannabinoid receptor-2 (CBR2). Moreover, tumour aggression and a poorer prognosis correlate with over-expression of CBR2 (Tavčar Kunstič, Debeljak and Fon Tacer, 2023). Cannabinoid receptors (CBRs), Peroxisome Proliferator-Activated Receptors (PPAR) and Transient Receptor Potential (TRP) channels are also expressed on immune system cells. These are target receptors of phytocannabinoids found in *Cannabis sativa* and for modulation of inflammatory pathways observed in both breast cancer and arthritis (Kisková *et al.*, 2019). For instance, Tetrahydrocannabinol (THC) treatment suppressed immune cell-mediated inflammation via inhibition of NF-κB, MAPK, and Janus Kinase-Signal Transducer and Activator of Transcription (JAK-STAT) inflammatory signalling pathways (Kisková *et al.*, 2019). Cannabidiol (CBD) decreased the survival of TNF-stimulated Rheumatoid Arthritis Synovial Fibroblasts (RASFs) by activating upregulated Transient Receptor Potential Ankyrin 1 (TRPA1) channels (Lowin *et al.*, 2020). While Cannabidiolic Acid (CBDA) exhibited anti-inflammatory effects in MDA-MB-231 by inhibiting COX-2 expression via regulation of PPAR signalling (Hirao-Suzuki *et al.*, 2020).

The *Cannabis sativa* plant has anti-inflammatory and antitumour properties that infer its great therapeutic potential against triple-negative breast cancer and rheumatoid arthritis. Through both CBR-dependent and independent mechanisms, individual phytoconstituent cannabinoids in *C. sativa* have been proven to suppress inflammatory cytokine production (Nagarkatti *et al.*, 2009). In addition, cannabinoids inhibit cancer cell proliferation and block inflammation-linked mechanisms, including COX-2 and MAPK signalling (Kisková *et al.*, 2019). Although it is evident that there are many possible biological targets, this study focused particularly on quantitatively monitoring the effects of *C. sativa* on PGE2 and nitrite expression; the qualitative effect on COX-2, IL-6 and TNF-α expression; as well as the antiproliferation effects on triple-negative breast cancer cells and inflammatory LPS-induced macrophages.

1.4 Aim

This study aimed to assess the modulatory effect of *Cannabis sativa* extracts on triple-negative breast cancer and rheumatoid arthritis progression and the expression of inflammatory bio-markers common in both conditions.

1.5 Objectives

a. To extract *Cannabis sativa* (biomass) and analyse the *C. sativa* extracts for cannabinoid content using LC-MS.
b. To examine the anticancer and anti-arthritic activity of *C. sativa* extracts in (MDA-MB-231) triple-negative breast cancer cell lines and LPS-induced RAW 264.7 macrophages representing inflammatory cells in cancer and arthritic microenvironments using the MTT assay.
c. To assess the anti-inflammatory and immunomodulatory activity of *C. sativa* extracts by screening post-treatment levels of COX-2, PGE2, nitrites, IL-6 and TNF-α in LPS-activated RAW 264.7 macrophages.

CHAPTER 2: LITERATURE REVIEW

2.1 *Cannabis sativa* (L)

2.1.1 Taxonomy and Traditional Use

The dioicous plant genus *Cannabis sativa* belongs to the Cannabaceae family (Pellati *et al.*, 2018; Farinon *et al.*, 2020) and has origins in Asia and Europe (Pellati *et al.*, 2018; Farinon *et al.*, 2020). It is characterised by an extremely diverse group of phenotypes, but due to taxonomical neglect, the classification recorded in literature is inconsistent (Pellati *et al.*, 2018; Balant *et al.*, 2021). Some individuals identify three species: fibre-type *C. sativa* L., high Δ9-THC drug-type *C. indica* Lam., and intermediate *C. ruderalis* Janisch.; or only recognise two species among these (C. *sativa* and C. *indica*.). The most commonly used nomenclature only recognises *Cannabis sativa* (L) as the primary species, which is further divided into different sub-species and varieties (Pellati *et al.*, 2018; Balant *et al.*, 2021). Based on use, there are industrially used hemp/fibre-type *C. sativa* and medicinally used marijuana/drug-type *C. sativa* (Farinon *et al.*, 2020; Balant *et al.*, 2021). However, according to chemical phenotypes, there are three principal chemotypes, namely type I, which is THC (psychoactive compound) dominant (>0.3%), fibre-type III, which is CBD (non-psychoactive) prevalent (<0.3% THC), and the intermediate type II, characterised by a slightly higher CBD/THC ratio (Farinon *et al.*, 2020).

Knowledge of *Cannabis sativa* historical benefits demonstrated in **Figure 1** below, spans over centuries in different geographical locations and is based on varying parts of the plant. For instance, seeds comprised human diet, particularly in Asia, while fibre was used to make various materials (clothing, rope, nets) predominantly in the western world (Farinon *et al.*, 2020; Balant *et al.*, 2021). The *C. sativa* plant was indigenously utilised to treat conditions such as pain, constipation, malaria and it was administered as a surgical anaesthetic together with wine in China (Pantoja-Ruiz *et al.*, 2021). The plant was also used to perform religious rituals and more importantly, to treat a wide range of ailments (Farinon *et al.*, 2020; Balant *et al.*, 2021). These uses are still applicable in present-day society, with medicinal use being the most relevant in the pharmacological industry. In the past, the whole plant was considered useful in

traditional medicine applications- for example, *C. sativa* roots were consumed specifically to treat cancer, arthritis, inflammation and joint pain. Recently, studies have highlighted an abundance of bioactive chemicals (monoterpenes, sesquiterpenoids, flavonoids and cannabinoids) in glandular trichomes of inflorescences and the leaves, to a lesser extent. Therefore, pharmaceutical research primarily uses these compounds (Booth and Bohlmann, 2019; Balant *et al.*, 2021).

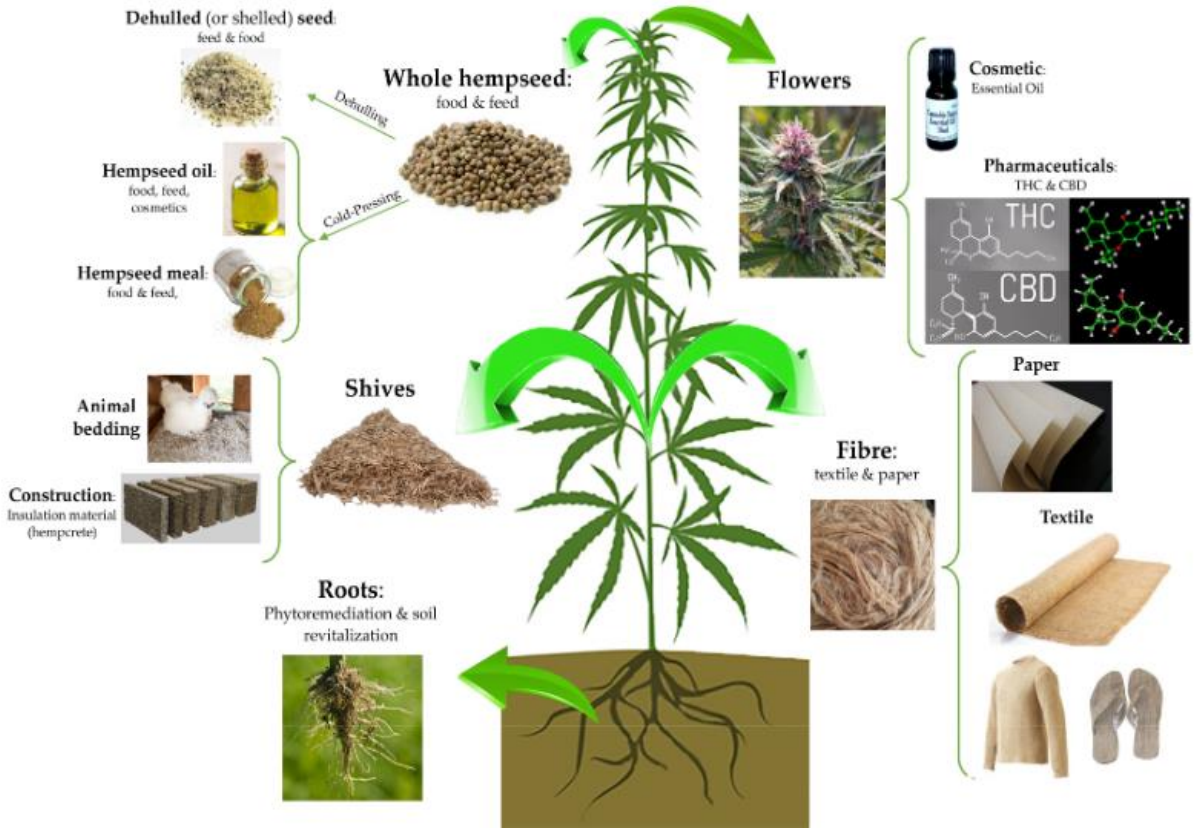

Figure 1: The myriad of domestic and commercial uses of *Cannabis sativa* (source: Farinon *et al.*, 2020)

Currently, *Cannabis sativa* has been used to develop treatments to alleviate inflammation and manage cancer and chronic pain (Balant *et al.*, 2021). However, little progress has been made in the innovation of more disease-specific drugs due to the complexity and wide chemical profile differences among strains and cultivars dependent on genetics, cultivation and harvesting conditions (Balant *et al.*, 2021), as well as the negative perception surrounding recreational use that exploits *C. sativa*'s addictive, intoxicating effects (Farinon *et al.*, 2020). Furthermore, although crude extracts are deemed medically superior compared to single compounds, the plant diversity results in major challenges when comparing results in preclinical and clinical

studies and standardisation of *C. sativa* products (Balant *et al.*, 2021).

2.1.2 Chemistry and Endocannabinoid System (ECS) Interaction

The complexity of *Cannabis sativa* is reinforced by its makeup, consisting of over 500 compounds (Aizpurua-Olaizola *et al.*, 2014). Although present phytochemical constituents include flavonoids, terpenoids, alkaloids, lignans, stillbenoids and essential nutrients (amino acids, fatty acids, vitamins and sugars), *C. sativa*'s prominence in pharmacology research is primarily due to cannabinoids (Lal *et al.*, 2021; Legare, Raup-Konsavage and Vrana, 2022), of which over 100 phytocannabinoids have been found in the *C. sativa* plant (Farinon *et al.*, 2020; Legare, Raup-Konsavage and Vrana, 2022). As demonstrated in **Figure 2**, they are naturally produced in their unstable acidic forms and then converted to neutral homologues through heating, decarboxylation, oxidation and isomerisation processes. Cannabigerolic acid (CBGA) is the major acidic precursor for CBDA and Tetrahydrocannabinolic Acid (THCA), which transform into CBD and THC, respectively. The conversion is catalysed by CBDA and THCA synthases (Aizpurua-Olaizola *et al.*, 2014; Lal *et al.*, 2021). Individual cannabinoids present unique pharmacological effects by engaging different physiological components, specifically within the endocannabinoid system (ECS).

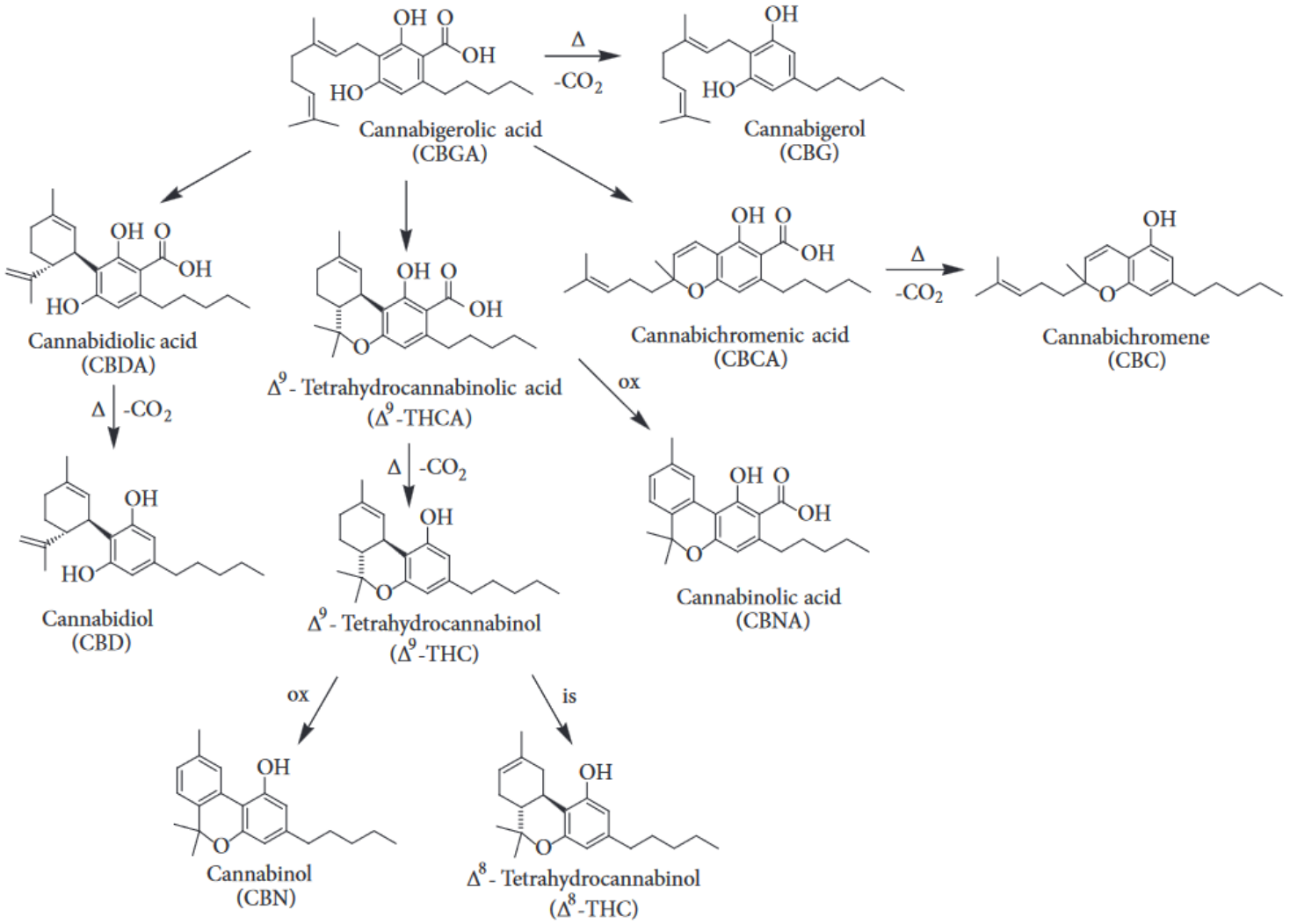

Figure 2: Pathway of biosynthesis of cannabinoids in *Cannabis sativa* (source: Pellati *et al.*, 2018). **Legend**: Δ= heating, -CO_2= decarboxylation, ox= oxidation and is =isomerisation.

The ECS is made up of endogenous ligands, including endocannabinoids, metabolizing enzymes and cannabinoid receptors (CBRs)- CBR1 and CBR2 (Legare, Raup-Konsavage and Vrana, 2022). The ECS acts on a wide range of body systems, including and beyond the nervous system and regulates several cellular processes such as cell growth and proliferation. Moreover, CBR targeting is connected to modification of various disease states (Zagzoog *et al.*, 2020; Legare, Raup-Konsavage and Vrana, 2022). For instance, ligands anandamide or N-arachidonoyl ethanolamine (AE) and 2-arachidonoyl glycerol (2-AG) by binding to CBR1, have portrayed cytotoxicity against cancer cells and suppressed metastasis (Lal *et al.*, 2021). Synthesis and degradation of endocannabinoids along with CBR activity can be influenced by exogenous cannabinoids (Legare, Raup-Konsavage and Vrana, 2022). In addition, besides through CBRs, these cannabinoids mediate physiological processes by interacting with other G protein-coupled receptors (GPCRs), orphan GPCRs, TRP channels, receptor families of PPAR, adrenoceptor and serotonin (5HT) receptors (Zagzoog *et al.*, 2020; Legare, Raup-Konsavage and Vrana, 2022). **Figure 3** below illustrates cannabinoid signalling via CBRs (Legare, Raup-Konsavage and Vrana, 2022).

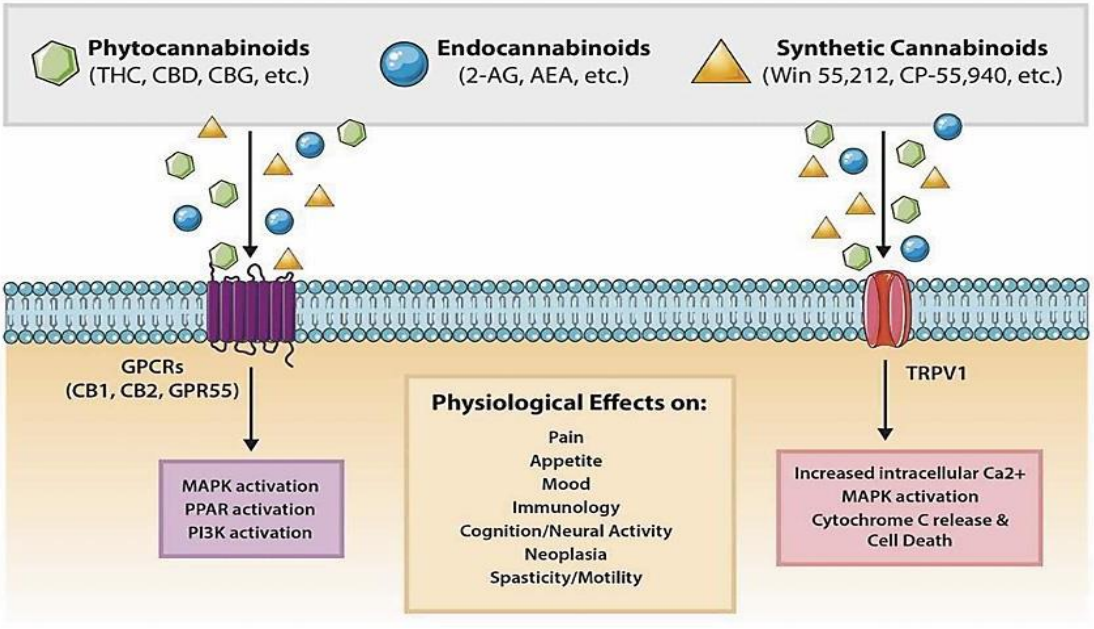

Figure 3: Cannabinoid signalling pathways and molecular and physiological effects (source: Legare et al., 2022)

In *Cannabis sativa*, CBD and THC are the most well studied cannabinoids with relation to the ECS. THC is primarily psychoactive and modulates inflammation, pain, and appetite mainly by binding CBRs. THC isomers Δ8-THC and Δ9-THC are partial agonists of CBR1 and CBR2; however, the former is more stable, while the latter is only stable in crude form. In its pure form, Δ9-THC readily oxidises to cannabinol (CBN) (Aizpurua-Olaizola *et al.*, 2014; Lal *et al.*, 2021). While Δ9-THC activation of CBR2 is linked to anti-inflammation, partial agonism at CBR1 is associated with analgesic, appetite-stimulating, antinausea and mood-altering effects (Zagzoog *et al.*, 2020). In contrast, CBD is known to possess neuroprotective properties that can regulate unwanted psychotropic effects of THC. CBD also generates anticancer, anti-diabetic (Aizpurua-Olaizola *et al.*, 2014), anti-inflammatory, anti-nociceptive, and anti-convulsant activity. CBD shows negative allosteric modulation and antagonism or inverse agonism at CBR1 and CBR2, respectively. However, it has lower affinity for ECS receptors compared to THC and thus largely acts externally to the ECS (Pellati *et al.*, 2018; Zagzoog *et al.*, 2020; Legare, Raup-Konsavage and Vrana, 2022). This includes being a 5HT-3A and GPR-18 and -55 antagonist; PPARγ, adenosine 1A and, 5HT-1A and -2A partial agonist as well as a mu (μ-) and delta (δ-) opioid receptor allosteric modulator (Zagzoog *et al.*, 2020).

Other minor cannabinoids and non-cannabinoids in *Cannabis sativa* have been reported to possess therapeutic effects (shown in **Table 1**). They may also play a synergistic role called the entourage effect, in which they potentiate the therapeutic efficacy of major constituents (Aizpurua-Olaizola *et al.*, 2014; Blasco-Benito *et al.*, 2018; Legare, Raup-Konsavage and Vrana, 2022). Similarly to CBD, terpenes can modulate Δ9-THC analgesic and psychotic effects by increasing permeability of the blood-brain barrier, changing affinity for CBR1 and through neurotransmitter receptor interaction. Flavonoids influence Δ9-THC pharmacokinetics by inhibitory action on cytochrome P450 liver enzymes (3A11 and 3A4) (Pellati *et al.*, 2018).

Table 1: Chemistry and Bioactivity of minor cannabinoids and non-cannabinoids found in *Cannabis sativa*.

Compound	**Class**	**Biochemical/ physiological effects**
Cannabigerol (CBG)	Cannabinoids	- Anti-proliferative, bone-stimulant (Aizpurua-Olaizola *et al.*, 2014), anti-tumourigenic via TRPM8 receptors (Blasco-Benito *et al.*, 2018), anti-analgesic, anti-microbial, anti-inflammatory (Pellati *et al.*, 2018) - *In-vitro* weak partial agonist at CBR1 and CBR2 with low cAMP suppression and pro-βarrestin recruitment (Zagzoog *et al.*, 2020). - *In-vivo* (Huntington's, multiple sclerosis, Parkinson's, and amyotrophic lateral sclerosis mouse models) poor anti-nociceptive, anxiolytic-like effects via TRP channels, GPR55, 5HT1A, and α2 adrenoceptor and PPARγ dependent disease mitigating anti-inflammation (Zagzoog *et al.*, 2020).
Cannabinol (CBN)		- Sedative (Aizpurua-Olaizola *et al.*, 2014), psychotropic and anti-proliferative (Lal *et al.*, 2021)
Tetrahydrocannabivarin (THCV)		- *In-vitro* weak partial CBR1 agonist and CBR2 agonist of cAMP inhibition and recruitment of βarrestin2 (other studies show CBR1 antagonism) (Zagzoog *et al.*, 2020).

		- *In-vivo* CBR dependent hypothermic, anti-nociceptive, anti-hyperalgesia, hypolocomotive, anxiolytic, neuroprotective, anti-epileptic, anorexic (Aizpurua-Olaizola *et al.*, 2014; Zagzoog *et al.*, 2020) - Clinical migraine treatment (Aizpurua-Olaizola *et al.*, 2014)
Tetrahydrocannabinolic acid (THCA)		∆9-THCA; - *in-vitro* cAMP production inhibition via CBR1 weak partial agonism and cAMP accumulation via weakly potent CBR2 agonism (Zagzoog *et al.*, 2020) - *in-vivo* anti-nociceptive via CBR1 agonism, anti-inflammatory and neuroprotective via CBR1, PPAR-γ (arthritis rodent model) and CBR2, as well as hypolocomotive and anxiolytic, (Blasco-Benito *et al.*, 2018; Zagzoog *et al.*, 2020)
Cannabidiolic acid (CBDA)		- *In-vitro* CBR2 weak partial agonism (Zagzoog *et al.*, 2020) - *In-vivo* 5HT1A mediated hypolocomotive, anxiolytic, anti-nausea and inflammatory pain reducing effects (Zagzoog *et al.*, 2020) and anti-microbial (Pellati *et al.*, 2018)
Cannabidivarin (CBDV)		- *In-vitro* partial agonist at CBR2 opposing cAMP generation and weak βarrestin2 recruitment (Zagzoog *et al.*, 2020)

		- *In-vivo* anti-convulsant at high concentrations (200–400 mg/kg p.o.) (Zagzoog *et al.*, 2020) - Anti-nausea and anti-microbial (Pellati *et al.*, 2018)
Cannabichromene (CBC)		- *In-vitro* CBR2 partial agonism resulting in membrane polarisation (Zagzoog *et al.*, 2020) - *In-vivo* enhanced neuron viability by ERK phosphorylation, inflammation and hypermobility reduction via TRPA1 and CBR independent anti-nociceptive and hypolocomotive effects (Zagzoog *et al.*, 2020)
Cannflavin A	Flavonoids	- Anti-inflammatory, good antileishmanial and a moderate antioxidant action (Pellati *et al.*, 2018)
Cannflavin B		- Anti-inflammatory, antimicrobial and antileishmanial (Pellati *et al.*, 2018)
canniprene		- Inhibited pro-inflammatory eicosanoids production through the 5-lipoxygenase (5-LO) pathway (Allegrone *et al.*, 2017).
β-myrcene	Terpenes	- Anti-inflammatory, analgesic, and anxiolytic (Pellati *et al.*, 2018)
β-caryophyllene		- anti-inflammatory, gastric cytoprotective and cannabinoid-like (binds CBR2) (Pellati *et al.*, 2018)

2.1.3 Clinical Applications and Regulations

Regulatory bodies such as the Federal Drug Administration (FDA) and European Medicines Agency (EMA) have approved a few *Cannabis sativa*-derived medications for medical use as a result of numerous pre-clinical and clinical studies on *C. sativa* effectiveness and safety (Legare, Raup-Konsavage and Vrana, 2022). Orally administered Δ9-THC analogs, such as Dronabinol (Marinol®) and Nabilone (Marinol®), are indicated for chemotherapy-induced nausea and vomiting (CNIV). The former also treats anorexic patients and Human immunodeficiency virus/Acquired immunodeficiency syndrome (HIV/AIDS) patients experiencing weight loss. Rimonabant (Acomplia®) was released to European markets after EMA approval for managing weight, dyslipidaemia, and diabetes, but retracted in 2009 due to its serious negative side effects. Nabiximols (Sativex®) is an oromucosal spray that treats spasticity in Multiple Sclerosis (MS), for instance, and contains Δ9-THC and CBD in roughly equal amounts. Cannabidiol/Epidiolex is a rigorously tested 98% pure plant-extracted CBD solution that is orally administered to children with Dravet syndrome or Lennox-Gastaut syndrome-related seizures. Significant analgesic effects were recorded in patients with neuropathic chronic pain, with nabilone being the most effective, followed by nabiximols, more so in peripheral neuropathy than centrally arising neuropathy, which is seen in disorders such as arthritis (Legare, Raup-Konsavage and Vrana, 2022).

Currently, numerous trials are underway to treat various diseases using various *Cannabis sativa* preparations, including single or a cocktail combinations of purified ingredients and crude extracts (Legare, Raup-Konsavage and Vrana, 2022). Some of the research is studying *C. sativa* as an adjuvant with standard drugs in conditions such as breast cancer. Evidence suggests that *C. sativa* and its constituents can modulate various biological processes (Legare, Raup-Konsavage and Vrana, 2022).

Cannabis sativa is recognised by the National Cancer Institute (NCI) and used as a palliative treatment against cancer symptoms and chemotherapy-associated side effects such as nausea, vomiting, pain, appetite loss and anxiety (Pellati *et al.*, 2018; Schoeman *et al.*, 2022). It has also been administered to advanced stage breast cancer patients (Kisková *et al.*, 2019).

2.2 Chronic inflammation

Chronic inflammation is involved in the pathogenesis of both cancer and arthritis. In cancer, prolonged inflammatory stimuli perpetuate a microenvironment that drives tumorigenesis, immune evasion, angiogenesis, and metastasis of cancer cells (Danforth, 2021). This chronic state involves the interaction of immune cells and inflammatory mediators (cytokines, ROS), leading to mutations and the survival and increased growth of malignant cells. Similarly, in autoimmune diseases such as rheumatoid arthritis, chronic inflammation results from an abnormal immune response that damages resident tissues and disrupts immune tolerance. Various genetic and environmental factors are responsible for sustained inflammation and disease progression (Mariani *et al.*, 2023; Sarzi-Puttini *et al.*, 2024).

In both hormone-receptor positive and triple-negative breast cancer, inflammatory pathways within the tumour microenvironment determine the properties of the cancer. Local cytokine signals emitted in the tumour microenvironment of triple-negative breast cancer can polarize abundant tumour-associated macrophages (TAMs) into either an anti-tumour M1 or pro-tumour M2 phenotype. ROS and cytokines such as IL-6 and TNF-α that induce oxidative stress and enhance cell proliferation attract immunosuppressive M2 macrophages. Through the release of pro-inflammatory mediators, obesity and the presence of crown-like structures in breast tissue contribute to this inflammatory environment and increase the risk of developing cancer. Additionally, the chronic inflammatory environment encourages resistance to treatment, especially in aggressive types of breast cancer such as triple-negative breast cancer (Danforth, 2021; Villarreal-García *et al.*, 2022).

One example of the damaging effects of persistent inflammation in autoimmune diseases is rheumatoid arthritis. The disease mainly affects the synovium, which is made up of immune cells such as synovial fibroblasts, macrophages, and T and B lymphocytes that work together to produce matrix-degrading enzymes and pro-inflammatory cytokines (e.g., TNF-α, IL-6). The synovial structure and extracellular matrix (ECM) develop into pannus, an aggressive tissue that breaks down bone and cartilage. The heightened immune response is caused by genetic factors, including HLA-DRB1 alleles, and epigenetic modifications. The inflammatory cycle is maintained by altered synovial fibroblasts. Despite advancements in treatment, central

sensitization and non-inflammatory mechanisms are linked to the persistent pain experienced by many rheumatoid arthritis patients, even when the inflammation is under control (Cheng, Liao and Wu, 2022; Mariani *et al.*, 2023).

2.3 Breast cancer

2.3.1 Pathogenesis

Cancer continues to be one of the leading causes of death globally. The biggest challenge to the successful treatment of cancer is the fact that cancer cells resemble normal healthy cells in various ways; hence, it is challenging to develop target-specific treatments (Berger and Mardis, 2018). The current most effective and safe approach involves identifying and targeting features unique to the cancer of interest, and this requires a thorough understanding of mechanisms driving cancer initiation and progression (NCI, 2021).

Triple-negative breast cancer is challenging to manage due to its high invasiveness as well as its recurrence, in contrast to other forms of breast cancer, and the associated lack of effective and tolerable treatment options. Unlike other subtypes with more favourable prognoses, triple-negative breast cancer does not express PR and ER and expresses low levels of HER2 (Yin *et al.*, 2020; Won *et al.*, 2022). It is a heterogenous disease and is generally classified based on genotypic profiling complemented by molecular subtyping or classification by mRNA expression. According to Lehmann *et al.* (2011), categorization that matches each type to a representative cell line model indicates six types: “basal- 1 (BL1), BL2, mesenchymal (M), mesenchymal stem-like (MSL), immunomodulatory (IM) and luminal androgen-receptor (LAR)” (Lehmann *et al.*, 2011). The MDA-MB-231 cell line belongs to the MSL subtype characterised by minimum proliferation gene levels but overexpresses HOX genes, stemness-related genes, mesenchymal stem cell specific markers, and receptors associated with angiogenesis (Yin *et al.*, 2020).

2.3.2 Role of Inflammation in Breast Cancer

The development of cancer is a multi-step process that starts with an initiation stage involving preneoplastic lesion formation. Over time, the lesion transforms into a

malignant tumour which can be triggered by intrinsic genetic factors and/or environmental exposure to carcinogens (biological- microbial infections, chemical- tobacco or alcohol consumption; physical- ultraviolet radiation) or ageing (Pellati *et al.*, 2018). Rudolf Virchow first identified the link between inflammation and cancer in the 19th century when he observed leukocytes inside tumours (Singh *et al.*, 2019). Inflammation in cancer can be either tumour-extrinsic in which the external factors associated with high cancer-risk (carcinogens, autoimmune disease, obesity) result in inflammation that can lead to malignancy, or intrinsic- carcinogenic mutations promote recruitment and activation of immune cells that can induce inflammation and thus create a tumour-nurturing inflammatory microenvironment (Singh *et al.*, 2019). Even in the absence of cancer-causing agents, chronic inflammation is predicted to play a role in 20% of malignant cancers. This means that cancer can induce inflammation and it can be induced by inflammation; thus, both carcinogenesis and inflammation most likely share common pathways (Pellati et al., 2018).

The intrinsically directed inflammation microenvironment comprises tumour-associated immune cells (dendritic cells, macrophages and lymphocytes) and the regulatory molecules they secrete, such as proinflammatory cytokines, growth factors, and chemokines, which promote cancer cell survival (Pellati *et al.*, 2018; Singh *et al.*, 2019). For example, chemotherapy resistance is endowed by activation of the pro-inflammatory pathway NF-kB and Epidermal growth factor (EGF) signalling (Pellati *et al.*, 2018). Some proinflammatory cytokines that have been detected in breast tumours are TNF-α, interleukins IL-10, IL-1, and IL- 6 (Singh *et al.*, 2019).

2.3.3 Treatment for Breast Cancer

As triple-negative breast cancer is unresponsive to standard targeted breast cancer medication, chemotherapy is currently the most reliable form of treatment for it. Examples of drugs include growth factor, Mechanistic Target of Rapamycin (mTOR), Phosphoinositide 3-Kinase (P13K), MAPK and Scr inhibitors. However, to enhance the poor efficacy of the few chemotherapeutic options, neoadjuvant regimens are also employed (Yin *et al.*, 2020).

2.3.4 *Cannabis sativa*, cannabinoids and anti-cancer activity

Cannabis sativa, and its cannabinoids, can contribute to breast cancer therapy through a wide range of signalling pathways that moderate not only inflammation and immune cell activity but also cancer cell proliferation, all of which are overlapping processes simultaneously involved in tumour onset and progression (Singh *et al.*, 2019). Cannabinoids have been documented to produce anti-cancer effects by mediating progression in different stages (uncontrolled cell division, survival, migration and angiogenesis) (Blasco-Benito *et al.*, 2018). Previous *in-vitro* and *in-vivo* breast cancer studies have primarily focused on pure cannabinoids, while few have explored the potential synergistic anti-cancer activity of by whole plant extracts or intentionally designed formulations that may increase efficacy (Blasco-Benito *et al.*, 2018).

Researchers have discovered that cannabinoids influence immune cells through both cannabinoid receptor-dependent and independent mechanisms, aiding in the disruption of pathologic inflammation within the breast cancer tumour microenvironment. CBR2 is the main cannabinoid receptor highly expressed by immune cells (Rodríguez Mesa *et al.*, 2021). It was also observed that highly metastatic MDA-MB-231 cells, representing the aggressive triple-negative breast cancer subtype, also express high levels of CBR2 and GPR55 receptors. Immunohistochemistry tests detected the immunoreactivity of CBR2 in 72% of human breast carcinoma samples versus 28% of CBR1, and no significant amount for non-transformed tissue. This expression is also linked to a poorer prognosis (Kisková *et al.*, 2019). CBR1 activation effects include G1/S phase stalling in breast cancer cells; thus obstructing cell cycle progression and the suppression of breast cancer cell migration by interrupting the FAK/SRC/RhoA pathway. CBR2 stimulation has similar effects; however, breast cancer cell cycle progression is blocked at the G2/M phase and migration is inhibited through COX-2 and Extracellular signal-regulated kinase (ERK) signalling, particularly in TNBC. Moreover, CBR2 activation was observed to moderate angiogenesis, induce cell death by activating the transcription factor jun-D, and inhibit the proliferation of breast cancer cells by suppressing the Akt/ERK signalling (Kisková *et al.*, 2019).

One study identified ROS generation in ER+ and ER- cells, which leads cancer-

selective induction of autophagy and apoptosis. The mechanism attributed was independent of CBRs and mainly involved ER stress, downregulation of the critical oncogenic signalling pathway AKT/mTOR/4EBP1, and mitochondria-mediated apoptosis (Shrivastava *et al.*, 2011). CBD, whose non-psychoactive nature makes it one of the most medically favoured cannabinoids, was found to induce apoptosis in CD4+ and CD8+ T-cells by increasing ROS synthesis and caspase 3 and 8 activity, and limited angiogenesis and tumour growth by suppressing cytokine secretion, resulting in less recruitment of immune cells by cancer cells (Kisková *et al.*, 2019). CBD also plays a therapeutic role through modulating growth factors, inflammation, and cell growth via suppressing the EGF/EGFR pathway, resulting in decreased macrophage recruitment in the tumour microenvironment, vascularisation and cancer cell migration (Pellati *et al.*, 2018). Another study using triple-negative breast cancer cells (MDA-MB-231 and MDA-MB-436) demonstrated CBD antiproliferative action and the suppression of triple-negative breast cancer invasiveness *in-vitro,* and downregulation of the overexpressed Fox M1 and ID-1, key proteins for cancer progression, was the proposed mechanism (McAllister *et al.*, 2007)

COX-2 enzyme is also a crucial component in inflammation processes and is highly expressed in metastatic breast cancers (~40%) (Takeda *et al*., 2012; Takeda *et al*., 2014); thus, making it a good biomarker and therapeutic target against aggressive breast cancer. Studies on CBDA, the main precursor for CBD, using the highly invasive triple-negative breast cancer model MDA-MB-231, provided evidence of the inhibitory activity of CBDA against COX-2. This selective COX-2 inhibition is mediated by inhibiting CAM-dependent pKA (protein kinase A) and Rho activation and results in a decrease in migratory activity (Takeda *et al*., 2012).

2.4 Arthritis

2.4.1 Rheumatoid Arthritis pathogenesis and inflammation

Rheumatoid arthritis is a chronic disorder resulting in joint swelling and pain due to autoimmunity and inflammation in the joint's synovial lining and deterioration of the bone and cartilage (Dudics *et al.*, 2018). It has the highest incidence in females and the elderly, but it can also begin during teenage years. Patients diagnosed with rheumatoid arthritis are categorised in two groups based on the presence of

rheumatoid factor (RF) in their serum; RF^- individuals test negative for RF and are said to have seronegative rheumatoid arthritis, while the majority, about 40 to 80 percent, are found to be seropositive (RF+) and often experience a more severe form of rheumatoid arthritis (Chang and Nigrovic, 2019). Different symptoms are also experienced at varying stages. The first pre- rheumatoid arthritis stage is associated with autoimmunity, followed by early rheumatoid arthritis, which occurs years later involving inflammation and articular onset, while more established rheumatoid arthritis presents with chronic inflammation and tissue damage (McInnes and Schett, 2017).

The pathogenesis of rheumatoid arthritis (illustrated in **Figure 5** below) is initiated by genetic and/or environmental factors that activate pathogenic T cells residing in the lymphoid organs or locally. First, autoantigens are presented by antigen-presenting cells (APCs) such as B-cells, to the abnormal autoreactive T-cells (Dudics *et al.*, 2018). The primed arthritogenic T-cells (Th1 and Th17) then disrupt the tolerance of normal regulatory T-cells (Th2 and Treg). Those from peripheral lymphoid organs chemotactically migrate to synovial tissue and together with the local T-cells, they secrete inflammatory mediators (TNF-α, IL-17, IFN-γ, and the receptor activator of nuclear factor KB ligand (RANK-L)), which activate fibroblasts and attract and stimulate pro-inflammatory cells such as macrophages (Dudics *et al.*, 2018). Macrophages are triggered to secrete even more proinflammatory cytokines, namely, TNF-α, IL-1β, and IL-6, which further perpetuate the inflammatory milieu. Meanwhile, RANKL, also produced by fibroblasts, facilitates osteoclastogenesis, in which macrophages differentiate into osteoclasts. Cartilage and bone degradation are mainly promoted by osteoclast and antibody action and activated articular chondrocyte and fibroblast-derived matrix metalloproteinases (MMPs) (Dudics *et al.*, 2018; Lin, Anzaghe and Schülke, 2020).

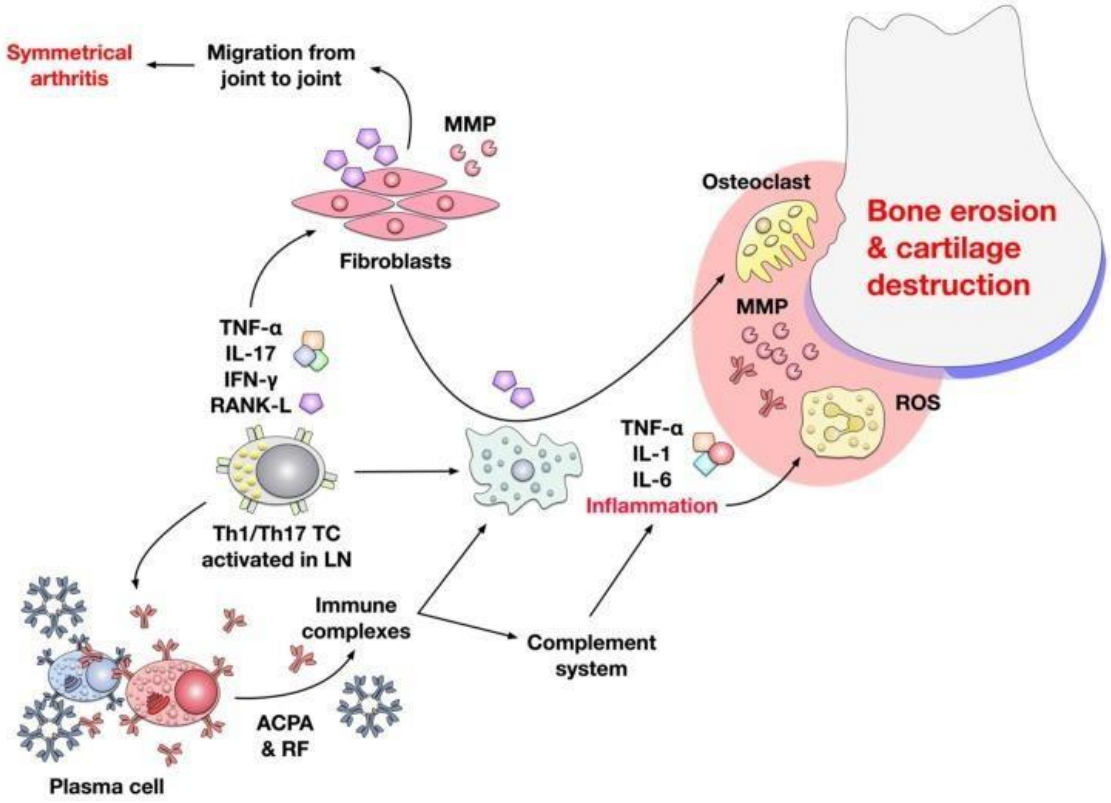

Figure 4: Mechanism of rheumatoid arthritis pathogenesis (source: Lin et al., 2020)

2.4.2 Treatment for Rheumatoid Arthritis

Common rheumatoid arthritis medications are categorised into non-steroidal anti-inflammatory drugs (NSAIDs) and biologic and chemical disease-modifying antirheumatic drugs (DMARDs). NSAIDs generally inhibit COX enzymes causing the suppression of prostaglandins. However, their side-effects, including renal, hepatic and cardiovascular toxicity are a major drawback. Methotrexate (MTX) is a gold standard rheumatoid arthritis drug whose mechanism of action comprises impeding proinflammatory cytokine production and regulating MMP levels (Dudics *et al.*, 2018). Unfortunately, MTX long-term use can result in the development of liver fibrosis, and it only has a 50% response rate among patients. Some popular biologic DMARDs, such as anti-TNF-α and anti-IL6R monoclonal antibodies, are immunosuppressive, making patients susceptible to infections. Anti-TNF-α is sometimes administered in combination with MTX due to some patients being unresponsive or losing responsiveness to the former over time. A more long-established group of biological DMARDs are corticosteroids; however, they also present adverse effects such as osteoporosis, peptic ulcers, and immunosuppression rates (Dudics *et al.*, 2018).

2.4.3 *Cannabis sativa* and anti-arthritis activity

Cannabis sativa possesses anti-inflammatory and analgesic activity that can alleviate arthritis symptoms, but very few studies have been conducted to test it as a potential arthritis drug candidate. Furthermore, these studies only concentrate on individual cannabinoids possessing anti-inflammatory activity, such as Δ^9-THCa and CBD, rather than crude extracts that allow for potentiating therapeutic effects between major and minor cannabinoids and other phytochemicals found in *C. sativa* (Kisková *et al.*, 2019). The presence of CBRs, especially CBR2 on peripheral immune cells, is the main feature allowing for *C. sativa's* anti-inflammatory and immunomodulatory effects against arthritis (Rodríguez Mesa *et al.*, 2021). Immune system cells are key drivers of inflammation in arthritis. The major population in rheumatoid arthritis includes macrophages, fibroblast-like synoviocytes, and dendritic cells, while key cytokines are TNF-α, IL-1 and IL-6 (Nagarkatti *et al.*, 2009; McInnes and Schett, 2017).

Cannabinoids also interact with non-cannabinoid receptors to drive anti-inflammatory processes. For instance, TRPV1 found on macrophages, dendritic cells and T-cells is overexpressed in association with inflammation and pain, and cannabinoid action is involved in moderating their proliferation, the secretion of cytokines, apoptosis, and the activation of T-cells. PPARs, specifically the isoforms PPAR-α and PPAR-γ, which are nuclear receptors, are also situated in B-cells, T-cells, and dendritic cells. The immunomodulatory effects of cannabinoid and PPAR interactions include changing cytokine secretion and lymphocyte proliferation (Rodríguez Mesa *et al.*, 2021).

Most studies on cannabinoid action against rheumatoid arthritis have given preference to non-psychoactive cannabinoids. An *in-vitro* study was also performed to test how rheumatoid arthritis synovial fibroblasts (RASF) would respond to CBD treatment. RASFs are suitable targets because they drive joint destruction by releasing enzymes involved in matrix degradation and pro-inflammatory cytokines. The study outcome showed that CBD “reduced cell viability, proliferation, and IL-6/IL-8 production of RASF” (Lowin *et al.*, 2020). In a murine model of arthritis, Δ^9-THCa's anti-inflammatory activity was dependent on CBR1 and PPAR γ *in vivo* (Zagzoog *et al.*, 2020).

Furthermore, in a collagen-induced arthritis (CIA) mouse model, CBD has been

demonstrated to considerably alleviate the disease progression. Its actions included inhibiting the proliferation of *ex-vivo* activated lymph node cells, lowering the secretion of IFN-γ, and reducing the synthesis of TNF-α by knee synovial cells (Malfait *et al.*, 2000). HU-320, a synthetic CBD analog, also ameliorated arthritis in mice (Sumariwalla *et al.*, 2004). In addition, experiments on human peripheral mononuclear blood cells (PMBCs) and fibroblast-like synovial cells (FLS) indicated that Ajulemic acid (AjA), a CBR2 agonist, reduced the synthesis of pro-inflammatory cytokines. AjA was also responsible for minimizing IL-1 production from peripheral blood and synovial fluid monocytes extracted from rheumatoid arthritis patients (Zurier *et al.*, 2003), as well as IL-6 from human monocyte-derived macrophages. Furthermore, it was found to potentially prevent osteoclastogenesis as it induces caspase 3 and 8 in mature osteoclast-like cells, which subsequently leads to apoptosis (George *et al.*, 2008).

Several preclinical research findings have indicated the anti-inflammatory action of other synthetic cannabinoids against rheumatoid arthritis. Examples include a FLS cell culture assay that showed a decline in pro-inflammatory cytokines IL-1, IL-6, and IL-8 after treatment with CP55, 940, and WIN55 (CBR1 agonist) (Selvi *et al.*, 2008), while C57BL/6 mouse FLS treated with the CBD analog O1821 and LER13 (both TRPV2 agonists) resulted in suppressed expression of MMP-2 and MMP-3 (Laragione *et al.*, 2015). Moreover, a bovine chondrocyte culture exposed to HU-210 (CBR1/CBR2 agonist) and WIN55 decreased extracellular matrix collagen and proteoglycan degradation in articular cartilage by lowering PGE2, inducible nitric oxide synthase (iNOS), COX-2, and NF-kB activation (Mbvundula *et al.*, 2006). In animal studies, C57B/6 mouse models administered with HU-320, a CBR1/CBR2 agonist, reduced the synthesis of TNF-α and reactive oxygen intermediates (ROIs) from macrophages (Sumariwalla *et al.*, 2004), while CIA mouse models dosed with HU-308 (CBR2 agonist) responded with a reduction in pro-inflammatory cytokines IL-6 and TNF-α in peritoneal macrophages (Gui *et al.*, 2015).

CHAPTER 3: METHODOLOGY

3.1 Ethical considerations

Ethical approval was obtained from the University of the Free State (UFS) Environmental Biosafety Research Ethics Committee (EBREC) before conducting the experiments outlined herein. The assigned ethical clearance number is **UFS-ESD2023/0223.**

3.2 Reagents

***Cannabis sativa* collection and extraction –** A sample of *Cannabis sativa* crude oil (Batch 0001) and spent biomass were provided by Prof. David Katerere and Mr Pollen Nkuna from the Tshwane University of Technology (TUT) and the Council for Scientific and Industrial Research (CSIR) hub, Pretoria, South Africa. The spent biomass was collected from Bushveld Genetics, Rustenburg, and was originally authenticated by Dr Manikandan Gurusamy (Pharmaceutical Sciences, TUT).

LC-MS - Dimethyl sulfoxide (DMSO), methanol and 1% methanol, mobile phase of 0.1% (v/v) formic acid acidified water (solvent A), 0.1% (v/v) formic acid acidified methanol (solvent B)

MTT Assay - 20 mg/ml of Crude *Cannabis sativa* extracts (SCF, hexane, acetone, methanol, E+H) and standard drugs (doxorubicin and methotrexate) stock solutions were prepared by weighing 20 mg of each and diluting it in 1 ml of DMSO or 1 ml of 1% ethanol for the E+H extract. These were stored in the 5 ℃ refrigerator until needed for various assays. Cell lines (MDA-MB-231, RAW 264.7 macrophages, and Vero) were maintained in the culture media and incubation conditions of 5% CO_2, 37 C and 95% humidity until the MTT experiment was complete and the cytotoxicity results of the various extracts were obtained. Gibco Dulbecco's modified eagle medium (DMEM 1×, [+] 4.5g/L D-Glucose, L-Glutamine, [+] Pyruvate) and foetal bovine serum (FBS) were used to prepare media to resuscitate (20% FBS in DMEM), to culture (10% FBS in DMEM) and to freeze (50% DMEM, 40% FBS and 10% DMSO) all the cell cultures (MDA-MB-231, RAW 264.7 macrophages, and Vero). Phosphate buffered saline (PBS) pH 7.4 (1×, Gibco) was used for washing the cells after discarding the spent media, trypsin for detaching cells, trypan blue to enhance countability, and 70% ethanol to maintain an aseptic working laboratory environment. Thiazolyl Blue Tetrazolium

Bromide 98% (Sigma Aldrich) was diluted to a concentration of 2.5 mg/ml and DMSO were used to perform an MTT assay on the treated and control cell groups.

Nitrite/ Greiss Assay - Contents of Invitrogen Griess reagent Kit (Thermo Fisher Scientific)- 0.1% (1 mg/mL) N-(1-naphthyl)ethylenediamine dihydrochloride solution (Component A), 1% (10 mg/mL) Sulfanilic acid in 5% phosphoric acid (Component B), Nitrite standard solution comprised of 1.0 mM sodium nitrite in deionized water (Component C). All components were kept in a 5°C refrigerator, away from light.

Prostaglandin E2 Enzyme-Linked immunosorbent assay (PGE2 ELISA) - Contents of Invitrogen PGE2 ELISA Kit (EHPGE2, Thermo Fisher Scientific) – Antibody Coated 96-well plate, reagent diluent, PGE2 antibody, PGE2-AP (Alkaline phosphatase-conjugated PGE2), PGE2 standard (50 000 pg/ml), 20× wash buffer, substrate solution, and plate sealer.

Western Blot Analysis

Protein extraction and quantification - Bicinchoninic acid (BCA) assay kit contents - 2 mg/ml bovine serum albumin (BSA), micro BCA reagent A (MA), micro BCA reagent B (MB) and micro BCA reagent C (MC).

Western Blot - RIPA lysis buffer was used for protein extraction and as a diluent for standardising protein samples to 50 µg/ml. Loading buffer was prepared by mixing 950 µl of 2× laemmli sample buffer (Biorad) and 50 µl denaturing β-Mercaptoethanol (β-ME) (Biorad). Running buffer comprised of 10× Tris/Glycine/SDS Buffer (Biorad) and dH_2O (1:9). The same combination was used to make washing buffer but with the addition of tween 20 (1:9:0.1). The buffers were stored in 500 ml and 2 L glass bottles and kept cool in a 5℃ refrigerator. Antibodies (0.006 mg/ml COX-2 monoclonal primary antibody (SP21) and anti-rabbit HRP-conjugated secondary antibody) were diluted in EveryBlot Blocking Buffer (Biorad). The Centrifuge 5804 R (Eppendorf) was employed for overnight incubation of the membrane with primary antibody. ECL (Enhanced Chemiluminescence) substrate solution was prepared by combining an equal volume of Clarity Western ECL substrate luminol/enhancer solution and Peroxide solution from BIORAD. Imperial Protein stain (thermo scientific, USA) was used for coomasie-blue staining of loaded gel after electrophoresis.

3.3 Procedures

3.3.1 *Cannabis sativa* collection and extraction

Two types of extracts were used i.e. Supercritical Carbon dioxide Fluid extract oil and spent biomass solvent extracts.

Supercritical Fluid (SCF) extract

A dried, milled *Cannabis sativa* flower biomass sample of the Durban Poison variety from Greenhouse Village weighing 4795 g was packaged into a nylon bag for SCF extraction. The SCF extraction system was operating on an automatic mode, set to a pressure of 210 bars and the extractor column temperature was kept at 60° to produce the SCF extract, also known as Full Extract Cannabis Oil (FECO).

Spent biomass extracts

The extraction of the spent biomass was performed according to a previously reported method (Lukhele and Motadi, 2016), with a few modifications. 500 g spent biomass consisting of ground *Cannabis sativa* flower, which was previously pre-extracted using supercritical CO_2 fluid (SCF) extraction, was sequentially soaked in 3 L of solvents by order of increasing polarity: n-hexane, acetone, methanol and a mixture of ethanol and distilled water (E+H) in a 1:1 ratio, placed on a shaker for 16 to 18 hours, and filtered. To maximize the purity and yield of the extracts, the extraction process was repeated twice with each solvent such that two samples of each extract were collected. The plant residue collected after filtration was mixed again with the same solvent. Before proceeding to the next solvent, the residue was laid out to air dry, and the filtrate of the respective solvent was concentrated through rotary evaporation. The resulting extracts were placed in a fume hood to further rid them of retained solvent and individually weighed to determine percentage yield. In contrast, the E+H sample was freeze dried after evaporating ethanol to avoid the extremely high temperature needed for water evaporation, which may compromise the structural integrity of the essential phytochemicals. A different plant sample was used to extract the *Cannabis sativa* crude oil. Percentage yield was calculated using the formula:

$$\textbf{Percentage yield} = \frac{\text{mass of crude extract (g)}}{\text{mass of plant material (g)}} \times 100\%$$

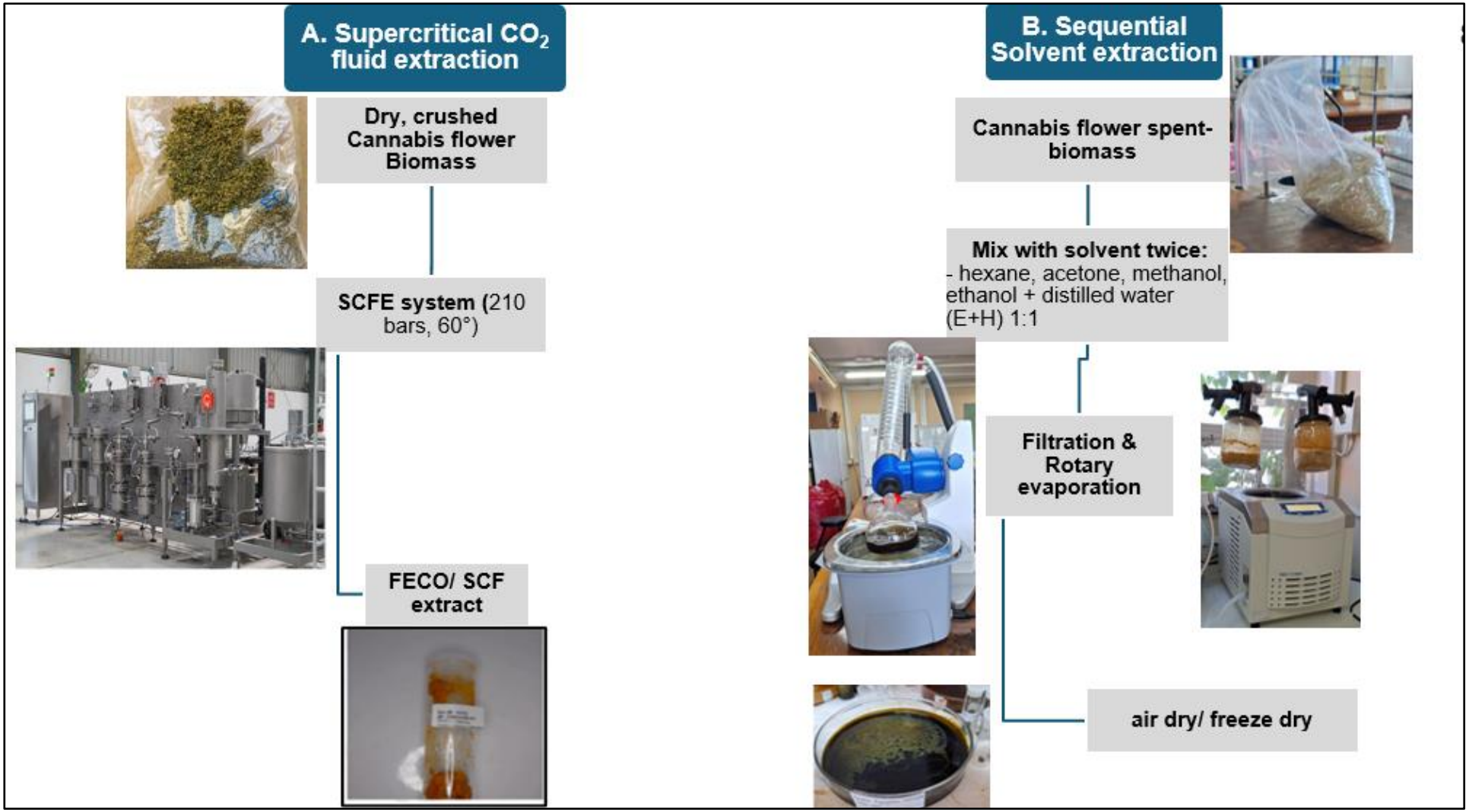

Figure 5: *Cannabis sativa* extraction procedure

3.3.2 LC-MS

LC-MS was carried out using the methodology as described by (Meng *et al.*, 2018) with a few modifications and available fragment masses from the literature as a reference. Stock solutions (10 mg/ml) consisting of 10 mg of each extract in 1 ml solvent were prepared – hexane, acetone, and supercritical SCF extracts were diluted in DMSO, while the E+H and methanol extracts were dissolved in 1% methanol in dH2O and pure methanol, respectively. Each sample was then diluted to 1 mg/ml by adding 100 µl stock solution in 900 µl methanol. Prior to injecting in the LC-MS column, the solutions were filtered using a nylon filter (0.45 µm pore size). Using the SCIEX OS software, the mass spectrometer acquisition method was set up as follows: the polarity was set to positive mode, individual compound positive ion precursor and product ion fragment masses (26 transitions) were input as displayed in Table 2 below. The separation and detection methods were optimized by adjusting the sample dilution, flow rate, column types, mobile phase gradient, and duration until the desired peaks (sharp and well separated) could be observed while the column temperature was kept constant at 40°C. Optimum extract separation, as observed by resulting total ion chromatogram (TIC) and Extracted-ion chromatogram (XIC) graphs, was obtained at 1000× dilution to avoid saturation of the detector by SFC extract, which had significantly higher cannabinoid concentrations, 10 µl Injection volume, 0.4 ml/min flow rate through the C18 column and gradient mobile phase of 60% B at 0 – 5 min, 95% A 5 – 7.5 min and 60% A 7.5 – 10 min, which allowed for good separation of the broad range of compounds being detected.

Table 2: Analyte (cannabinoid) chemistry and LC-MS profile information

Names and Chemical formulae	**Intact mass (g/mol)**	**Precursor Ions** (Citti *et al.*, 2019; McRae and Melanson, 2020)	**Product Ions (Citti *et al.*, 2019; Mcrae and Melanson, 2020)**
Δ^9THC ($C_{21}H_{30}O_2$)	314.5	315.2	259, 193, 135
CBD ($C_{21}H_{30}O_2$)	314.5	315.2	259, 235, 193, 269, 229
Δ^9THCA ($C_{22}H_{30}O_4$)	358.48	359.2	341, 313, 219
CBDA ($C_{22}H_{30}O_4$)	358.5	359.2	341, 313, 261
CBG ($C_{21}H_{32}O_2$)	316.48	317.2	193, 123
CBGA ($C_{22}H_{32}O_4$)	360.50	361.2	343, 261, 219
CBC ($C_{21}H_{30}O_2$)	314.5	315.2	245
CBN ($C_{21}H_{26}O_2$)	310.45	311.2	293, 241, 223
CBDV ($C_{19}H_{26}O_2$)	286.41	287.2	259, 235, 193

3.3.3 Cell Culture and MTT

3.3.3.1 Cell resuscitation

Three cryovials of preserved cells per cell line were obtained from the -80 ℃ refrigerator of the Pharmacology Laboratory at the University of the Free State. The cells were resuscitated in relevant media (gibco Dulbecco's Modified Eagle Medium 1×, [+] 4.5g/L D-Glucose, L-Glutamine, [+] Pyruvate), which was pre-warmed to 37 ℃ along with cryopreserved cells until small ice remained in the cryovials. Cell suspension from each vial was transferred into a centrifuge tube (15 ml) containing 3 ml media and centrifuged at 1500 rpm for five minutes. After discarding the supernatant, the cell pellet was resuspended in 1 ml media and pipetted into a T25 flask containing 5 ml media and incubated at optimum conditions (37 ℃, 95% humidity, 5% CO_2) until ~80 % confluency was reached. Media was regularly inspected for change of colour or contamination, and the cells were visualized under a microscope to assess attachment and confluency. Media was changed when the normal bright red-pink colour turned orange indicating that it was spent, by discarding the waste media, washing the flask with 3 ml PBS and replacing it with 5 ml of fresh media.

3.3.3.2 Sub-culturing

The cells were sub-cultured in culturing media. Once the cells had fully adhered and were ~ 80% confluent, the waste media was discarded, followed by washing with 3 ml (T25) or 5 ml (T75) PBS, and trypsinization for which PBS is replaced by the same volume of trypsin, incubated for three minutes, and quickly observed for detachment. The flasks were rapidly tapped on the bottom to aid detachment when necessary. Trypsin was then neutralized by adding media (4 ml- T25 or 6 ml- T75), followed by centrifuging the mixture at 1500 rpm for five minutes. The supernatant was discarded, replaced with 1 ml sub-culturing media, and the resuspended cell pellet was split into two T75 10 ml media containing flasks for each T25/ T75 flask. All reagents (media, PBS and trypsin) were pre-warmed to 37 ℃.

3.3.3.3 MTT assay

For MTT, extracts were diluted in cell culture media to 0.1, 1, 5, 10, 12.5, 25, 50, and 100 µg/ml.

MDA-MB-231 and Vero

Before proceeding with the MTT assay, cells were sub-cultured at least once and were required to have viability of ≥ 85%. This was determined by mixing 10 – 20 µl of the homogenous 1 ml cell suspension with an equal volume of trypan blue and transferring into a cell counter. The cells were then resuspended at a density of 1×10^5 cells/ml. 100 µl media and an equal volume cell suspension were transferred into 96 well plates for seeding.

After 24 hours, cell adherence was confirmed, media was discarded and replaced with 100 µl of the treatment dilutions or doxorubicin for the positive control or culture media alone for the negative control. A blank was represented by media without cells and treatment. After 48 hours incubation, supernatant was discarded, wells were washed with 100 µl PBS, replaced with 200 µl neat DMEM and 20 µl of 20 mg/ml MTT reagent and four hours incubation. The wells were then emptied and MTT formazan salt was solubilized by the addition of 100 µl DMSO and mixing by placing on a horizontal shaker for 10 minutes to produce a purple (for presence of live cells) or transparent (for absence of live cells) colour. The colour intensity, used to deduce cell viability after treatment or other conditions, was measured by taking absorbance readings at 560 nm. Three biological replicates were used for each control group and percentage cell growth inhibition was calculated using the following formula:

$$100\ \% - \left(\frac{Test\ group\ absorbance - Blank\ absorbance}{Negative\ control\ absorbance - Blank\ absorbance} \times 100\ \%\right)$$

RAW 264.7 macrophages

RAW macrophages followed a similar procedure as the MDA-MB-231 and Vero cells. However, after 24 hours of seeding, media was replaced by 1 µg/ml LPS and cells were incubated for 24 hours to allow stimulation, followed by only 24 hours with treatment. Additionally, methotrexate (MTX) was used as the positive control instead of doxorubicin. IC_{50} (half-maximal inhibitory concentration) values were calculated and used to determine the most potent extracts. However, IC_{10} (concentrations at which 10% growth inhibition is reached) of the selected extracts were used to treat stimulated macrophages in the subsequent anti-inflammation assays (Griess, ELISA and Western blot) to eliminate a false positive result of reduced cytokine expression due to cytotoxicity as opposed to suppressed production.

3.3.4 Nitrite/ Greiss Assay

For conducting the Greiss assay, seeding, LPS-stimulation, and the treatment of RAW 264.7 cells were performed in 24 well plates. First, 500 µl cell suspension of 1×10^5 cells/ml density was seeded and incubated for 24 hours to allow attachment, media was discarded and replaced with 500 µl of 1 µg/ml LPS for 24 hours to activate the cells. Next, for the treatment step, the most potent extracts (SCF and acetone); water-based E+H and MTX were added at their IC_{10} concentrations (SCF- 10.2 µg/ml, acetone- 8.80 µg/ml, E+H- 23.0 µg/ml, MTX- 1 µg/ml). Similarly to MTTtreatment-free media was added to the controls (only LPS induced and untreated) and all groups were left in the incubator for a final incubation period of 24 hours. Supernatant media for each group was transferred into Eppendorf tubes. According to the manufacturer's kit instructions, Greiss reagent was prepared by mixing equal volumes (1 ml) of N(1-naphthyl) ethylenediamine dihydrochloride and sulfanilic acid. Sodium nitrite ($NaNO_2$) standard was mixed with dH_2O to concentrations ranging from 0-100 µM. Standard dilutions and the collected samples of supernatant (150 µl) were transferred into 96 well plates in triplicates followed by the addition of 20 µl Greiss reagent and 130 µl dH_2O. A photometric reference sample consisting of 20 µl Greiss reagent and 280 µl dH_2O was also included. Then the plate was left to incubate at room temperature for 30 minutes. Lastly, absorbance was measured at a wavelength 560 nm and using the calibration standard curve of absorbance values of the standards versus their concentrations, nitrite concentration indicating the degree of inflammation in each sample was deduced.

3.3.5 PGE2 ELISA

The same steps were followed as for the nitrite assay up until the supernatant media for each group was transferred into Eppendorf tubes. According to the manufacturer's PGE2 ELISA kit manual, the kit components were left to thaw at room temperature for 30 minutes before use. 1× wash buffer was prepared by diluting 5 ml of the 20× buffer in 95 ml dH2O while the PGE2 standard was diluted with cell culture media to concentrations of 0, 39.1, 78.1, 156, 313, 625, 1250 and 2500 pg/ml. 100 µl of supernatant, standards, and culture media for blank and non-specific binding (NSB) samples were transferred into the antibody-coated well plate in triplicates. This was followed by the addition of 50 µl reagent diluent, blue PGE2-AP and yellow PGE2

antibody to NSB, to all wells except the blank, and to only standard and supernatant wells, respectively; thus, resulting in the observation of a blue colour in the NSB wells, while the other wells besides the blank appeared green. The plate was sealed and left to incubate on a shaker (200 rpm) at room temperature for two hours, after which the wells were emptied and washed three times with 400 µl wash buffer. Next, the buffer was thoroughly removed by tapping the plate on paper towels and 5 µl blue PGE2-AP was added to additional total activity (TA) wells. Next, 200 µl substrate solution was added to all the wells and after leaving the plate to incubate at room temperature for 45 min without shaking, 50 µl of the stop solution was added. Finally, absorbance readings were immediately taken at 405 nm. A PGE2 standard curve was constructed by plotting average net absorbance of the standard samples against their known concentrations, and then used to calculate the PGE2 concentration of the collected supernatant samples.

3.3.6 Western Blot Analysis

3.3.6.1 Protein Extraction

The procedure and incubation periods for seeding, LPS-stimulation and treatment of RAW 264.7 cells were carried out similarly to the Greiss assay method. However, 4 ml cell suspension was seeded in T25 flasks at a density of 2×10^{6} cells/ml until confluent and replaced with 4 ml 1 µg/ml LPS and 4 ml treatment or media only in the second and final incubation periods, respectively. After a PBS wash, three minutes incubation with 3 ml trypsin was applied for detachment. 4 ml media was added to neutralize trypsin protease and cells were suspended by centrifuging at 1500 rpm. The supernatant was discarded and from this point forward, the temperature was maintained below 5 °C. Cells were resuspended in 1 ml RIPA lysis buffer (Pierce, Reference 89900, Lot YF369700), incubated 30 minutes and centrifuged for 10 minutes at 4℃, 12000 rpm to extract protein. The supernatant containing protein was immediately collected and stored at - 20℃ until the analysis stage.

3.3.6.2 BCA assay

A BCA assay was performed using the micro-BCA protein assay thermofisher kit and protocol to determine concentrations of each control group in order to standardize for the Western blot. First, the samples were thawed in a controlled manner to prevent a rapid increase in temperature; thus, they were placed on ice in a container outside the -20 ℃ refrigerator. Meanwhile, standard dilutions of 2 mg/ml BSA protein were prepared by mixing in dH_2O to concentrations of 0, 5, 25, 50, 75, 250, 500, 750, 1000, 1500 and 2000 µg/ml. 10 ml BCA working reagent was also prepared by mixing 5 ml MA, 4.8 ml MB and 0.2 ml MC. Next, 150 µl of the samples and standards were pipetted in duplicates onto a 96 well plate, followed by 150 µl of the working reagent. The plate was placed on a shaker for 30 seconds for agitation; then, it was covered with biofilm and incubated at room temperature for three hours. This resulted in a purple colour change in the presence of protein – the more intense the colour, the higher the protein content. Intensity was measured by taking absorbance readings at 560 nm. Standard protein absorbance readings were used to create a standard curve of absorbance against concentration and generate a linear trendline of formula y = mx + c where y represents absorbance and x is concentration. By substituting the sample absorbance values, individual protein concentrations for each group were calculated.

3.3.6.3 Gel Electrophoresis and Western Blot

The gel electrophoresis and western blot protocol implemented was previously established by a colleague (Ms. Nandi Mabaso) for a completed Masters Pharmacology research project. Equal volumes of standardized protein samples (35 µl) and loading buffer (35 µl) were thoroughly mixed. To further ensure protein denaturation, the samples were heated at 95 ℃ for five minutes. An electrophoresis tank chamber was partially prefilled with running buffer. After removing, three gels were set up in the tank and left to soak for a few minutes in the running buffer to allow for the smooth removal of gel combs that would not break the wells. The tape at the bottom of the gel cassettes was also removed before assembling them back into the chamber. 20 µl of samples along with the protein ladder were loaded in triplicates, one replicate per gel. Electrophoresis was run at a constant 120 volts and a check for rising bubbles within the tank was conducted to verify that the run had begun. Once the protein dye front reached the gel reference line, the run was stopped. The gel was

taken out of the tank and gently removed from the cassette casing with gloved hands dipped in buffer and laid (ensuring that the front side where the dye and samples were loaded was facing up) onto the clean, slightly buffer-wetted imaging system platform and ironed out to remove ridges and bubbles. The gel was activated by selecting the stain free gel option (the image generated is shown in **Figure 1A** in the **appendix** section). Following this, **two** of the gels were individually placed in the transfer membrane stack (with the front side facing the top stack) then into the transfer-system to transfer protein bands. The membrane was incubated overnight at 4℃, with 10 µl primary COX-2 antibody diluted in 10 ml blocking buffer (1:1000) followed three washes with washing buffer, one hour incubation with 10 µl secondary HRP-conjugated antibody also diluted in 10 ml blocking buffer (1:1000) and three more washes. Lastly, the membrane was placed on the chemiDoc, ironed out, activated, and drops of ECL solution were added onto the membrane and spread out using the roller. The blot chemiluminescence option was selected to view COX-2 protein expression bands.

3.3.6.4 Coomasie-blue staining

The remaining gel was incubated for two hours in the imperial protein stain solution (just enough to completely cover the gel) on the orbital microplate mixer set at a low speed, at room temperature. It was followed up with similar incubation in dH_2O on the mixer overnight.

3.4 Statistical analysis

Apart from extract percentage yields and relative cannabinoid content, all data was collected in triplicates, outliers were eliminated, and the results are presented as mean ± standard deviation (SD). GraphPad Prism version 6 was used to determine statistical significance (**Figures A9, A11 and A13**). The data analysed included nitrite, PGE2 and protein concentration results. The means data of different treatment groups were compared using ordinary one-way Analysis of Variance (ANOVA) method and Tukey's multiple comparison's test. Ordinary one-way ANOVA was applied to determine if there were statistically significant differences between the means of the independent test and control groups for each experiment, while Tukey's post hoc test was conducted on significant ANOVA results to identify which specific groups differ

from each other. Differences were considered statistically significant at $p<0.05$.

CHAPTER 4: RESULTS AND DISCUSSION

4.1 *Cannabis sativa* extraction

Upon successful extraction, using two types of extracts, i.e. SCF and spent biomass extracts, various percentage yields were observed as highlighted in the **Table 3** and discussed below.

Table 3: Percentage yields of various solvent extract

SOLVENT	SAMPLE NUMBER	ORIGINAL PLANT MASS	EXTRACT MASS (g)	PERCENTAGE YIELD (%)	TOTAL PERCENTAGE YIELD (%)
HEXANE	**1**	500	5.76	1.15	1.65
	2		2.51	0.50	
ACETONE	**1**		11.4	2.29	3.22
	2		4.65	0.93	
METHANOL	**1**		19.8	3.96	5.78
	2		9.12	1.82	
E+H	**1**		24.6	4.92	7.51
	2		13.0	2.59	
SCF	N/A	4795	828	17.3	17.3

Table 3 shows the mass and percentage yields of the four extracts (two samples each) obtained from sequential solvent extraction of 500 g spent *Cannabis sativa* biomass and a single Supercritical Carbon dioxide extract sample from 4795 g of fresh, *C. sativa* flower. The percentage yields ranged from 1.65% - 17.3%. The extraction yield varied depending on the solvent used, for instance, sequential solvent extraction percentage yields increased with increasing solvent polarity, with the highest yield obtained by the most polar solvent- E+H (7.51%), while the lowest percentage was observed with the most non-polar solvent- hexane (1.65%). Each solvent was used on two different samples and typically, sample 1 had a greater yield compared to sample 2. The extensive solvent-based extractions collectively yielded a percentage of 18.2% plant extract, however, only one round of SCF extraction yielded a comparable percentage of 17.3%. Thus, SCF extraction showed a superior ability to extract a wider range of

compounds more efficiently than sequential solvent extraction. All extracts were collected and suitably stored for phyto-cannabinoid analysis and subsequent *in-vitro* studies as outlined in the methodology section. **Legend:** E+H= ethanol and water, SCF= supercritical carbon dioxide fluid, N/A= not applicable.

According to the percentage yield results in **Table 3**, extract yield for spent biomass extracts increased with the increasing polarity of solvent, such that the hexane extract was the least (~1.65%) and the E+H extract was the highest (~7.51%) obtained. The extract quantities decreased in the second rounds of extraction, indicating that some phytochemicals were still retained in the plant material even after the first extractions. As expected, the SCF extract obtained from unprocessed *Cannabis sativa* biomass yielded a greater percentage of 17.3% compared to the solvent-extracted samples which made use of previously extracted, spent-biomass. SCF extraction is considered more environmentally friendly and efficient as it employs food grade CO_2, which is less toxic compared to organic solvents, and produces substantial yields in a short time (Pino *et al.*, 2023).

Subsequent to extraction, the SCF and spent biomass extracts were analysed for the presence of cannabinoids, the relative percentages of various cannabinoids found in the extracts are displayed in **Table 4** and discussed below.

Table 4: LC-MS Analysis Relative Cannabinoid Content (%).

RT	**2.49**	**2.83**	**4.20**	**2.31**	**3.56**	**2.82**	**3.99**	**3.97**	N/A
	CBDA	**CBGA**	**THCA**	**CBG**	**CBD**	**CBN**	**THC**	**CBC**	**CBDV**
SCF	100	0.757	89.1	6.43	100	100	100	100	N/A
Hexane	6.41	97.5	100	100	73.6	21.7	40.0	45.9	N/A
Acetone	4.26	100	56.5	17.0	11.3	2.71	4.29	5.16	N/A
Methanol	0.265	3.23	5.97	0.886	N/A	0.780	N/A	5.85	N/A
E+H	0.0640	0.464	3.23	0.134	N/A	0.238	N/A	2.56	N/A

Table 4 summarises the relative cannabinoid quantity of the supercritical carbon dioxide fluid extract and the four sequential solvent extracts derived from *Cannabis sativa* plant material following LC-MS analysis. The retention time indicates the

duration it took for each identified cannabinoid to reach the chromatography detector from the point of injection of the extract sample. The unique LC-MS chromatogram generated by a given extract was used to find the relative quantity of the various cannabinoids of interest it contains, in order to determine if the assessed *in-vitro* effects of the extracts can be linked to their cannabinoid composition and abundance. For example, if extract A is more cytotoxic than extract B, perhaps a certain cannabinoid with cytotoxic properties is more concentrated in extract A than in extract B. Area under the curve (AUC) was calculated for respective peaks formed at a specific cannabinoid's retention time and this was expressed as a ratio of the highest AUC to calculate the relative cannabinoid percentage, using the formular below:

$$\frac{AUC_{extract}}{AUC_{highest}} \times 100$$

The above results indicate that SCF extraction yielded substantially high cannabinoid content across all compounds ranging between 89.1% - 100%, except for CBG (6.43%) and CBGA (0.757%). On the other hand, for the extracts obtained through to solvent extraction, non-polar solvents (hexane and acetone) extracted cannabinoids more efficiently than more polar solvents (methanol and E+H). Hexane effectively extracted CBG (100%) and acidic cannabinoids- THCA (100%) and CBGA (97.5%) and to a lesser extent- CBD (73.6%) and THC (40.0%). Similarly, acetone extracted acidic cannabinoids in high amounts (CBGA- 100% and THCA- 56.5%) however extraction of CBD (11.3%), CBN (2.71%) and THC (4.29%) was extremely low. In contrast, methanol and E+H showed very poor cannabinoid extraction ranging between 0.0640% (CBDA by E+H) and 5.97% (THCA by methanol). Thus, SCF extraction was the most effective method for extracting both acidic and neutral cannabinoids, hexane solvent demonstrated high affinity for acidic cannabinoids while polar solvents were least suitable for extracting cannabinoids.

Legend: RT= retention time, CBDA= Cannabidiolic Acid, CBGA= Cannabigerolic Acid, THCA= Tetrahydrocannabinolic Acid, CBG= Cannabigerol, CBD= Cannabidiol, CBN= Cannabinol, THC= Tetrahydrocannabinol, CBC= Cannabichromene, CBDV= Cannabidivarin, E+H= ethanol and water, SCF= supercritical carbon dioxide fluid, N/A=no distinct peaks observed in the ion chromatogram (XIC) graphs shown in **Appendix Figures A3-A7.**

Phytochemical analysis was conducted to identify the bioactive compounds in each extract. While the SCF sample was analysed using Potency *Cannabis sativa* High Performance Liquid Chromatography (HPLC) (test method TM006.3), GC-FID terpene analysis (test method TM003.5) conducted by the National Analytical Forensic Services (NAFS) (the Certificate of analysis results are provided in the appendix **Figure 2A**) and LC-MS, the other extracts only underwent LC-MS analysis. LC-MS can be applied in traditional medicine quality control as it allows for detecting and quantifying phytochemicals to standardise dosage for *in-vivo* use (Bala *et al.*, 2019). In comparison to other methods, LC-MS has been found to have better sensitivity and it can be used to analyse a diverse range of products, making it highly reliable. However, the LC-MS analysis in this instance was limited by the lack of cannabinoid standards. Isomer cannabinoids such as CBD and THC, were distinguished by established differences in retention time (Citti *et al.*, 2018, 2019). Without standards, it was also impossible to obtain the actual quantity or concentration of the cannabinoids in each extract, therefore only relative quantitation could be conducted.

The NAFS Certificate of Analysis (COA) report on the SCF extract revealed that it contains high amounts of THCA (~36.4 %), ∆9THC (~12.0 %) and CBGA (0.921 %), as well as trace amounts of several terpenes – nerolidol, β-pinene, linalool, guiaiol, limonene, α-pinene, β-myrcene, α-bisabolol, α-humulene and β-caryophyllene – with mass ranging from 0.832 - ~7.44 mg per 1 g extract (0.0832 - 0.744 %). However, essential cannabinoids such as CBC, CBD, CBG, CBD-V, THCV, CBN the precursor CBD-A were not detected.

The presence of the cannabinoids of interest and their retention times was first determined in the SCF extract using the available NAFS COA report as a reference in addition to theoretical ion fragmentation and elution patterns. According to Citti and co-authors (2019), LC-MS analysis revealed that elution of CBD-type cannabinoids starts with CBDV followed by CBDA and then CBD comes later due to its comparably high hydrophilicity. For the THC-type, ∆9-THC is known to be more lipophilic and therefore elutes after CBD and CBN, however, it elutes faster than its acidic precursor THCA. CBN was observed to elute between CBD and THC due to its higher lipophilicity and polarity, respectively. On the other hand, CBG-type cannabinoids CBG and CBGA

eluted closely to CBD and CBDA, respectively, as a result of possessing slightly different lipophilicity, while CBC elutes after THC and closely but prior to THCA (Citti *et al.*, 2019).

Similarly to Citti and fellow researchers (2019), based on the results illustrated in appendix **Figure A3,** THCA and CBDA showed matching spectra with definite peaks at retention times (RTs) 2.49 and 4.21 minutes. Given that previous studies show THCA elutes later (Citti *et al.*, 2019; Mcrae and Melanson, 2020), it was assigned a RT of 4.21 minutes, leaving 2.49 minutes for CBDA. However, the area under the curve (AUC) at 2.49 minutes was greater than at 4.21 minutes, which contradicts the NAFS report indicating CBDA was not detected. Suggesting that more CBDA may have been synthesised from available CBGA by preserved synthases in the crude extract (Zirpel, Kayser and Stehle, 2018). Again, the results showed identical spectra for THC, CBD and CBC. All three transitions of THC and the one transition of CBC formed peaks at four positions (distinct peaks at 2.24, 3.56 and 3.98 minutes and a split peak at 3.08). For CBD, two (269, 229) out of its five transitions were less prominent at all of the retention times. Considering the COA results showing that the SCF extract had higher amounts of THCA and THC than CBD and previous literature indicating that CBD is eluted first and is followed by THC and CBC in close proximity, it was determined that THC and CBC were eluted at 3.98 and CBD at 3.56, however, 2.24 minutes was eliminated as the retention time for CBD. CBGA and CBG had distinct peaks for both their transitions at only 2.34 and 2.48 minutes, respectively. No distinct peaks were seen for CBDV's chromatogram, which can be explained by its volatile nature. The LC-MS results affirmed the presence of THCA, ∆9THC and CBGA in the SCF extract. However, CBDA and CBG, which were undetected in the reported HPLC COA, were observed through LC-MS, attesting to its high sensitivity.

Organic solvent extraction confirmed that waste material from SCF extraction retains bioactive compounds with potential therapeutic application. The same retention times identified in SCF analysis were applied to the remaining extracts to obtain relative quantities of all cannabinoids of interest. Comparing the four extracts, hexane and acetone contained the highest amounts of all the tested cannabinoids, with THC, THCA, CBDA and CBG being the most abundant in hexane, while CBG was highest in the acetone extract. On the other hand, the cannabinoids were found to be

significantly lower in the E+H and methanol extracts. This is consistent with literature showing that cannabinoids are generally non-polar; hence, solvents with low polarity are most suitable for their extraction (Ubeed *et al.*, 2022).

Some studies have revealed that phytocomplex products, such as the SCF and the solid-liquid extracts from this study, are more desirable compared to isolated secondary metabolites due to potentiated bioactivity by the combined action of different constituents termed the “entourage effect” (Di Giacomo *et al.*, 2021; Pino *et al.*, 2023). However, the majority of studies so far have focused only on isolated compounds from *Cannabis sativa*.

4.2 MTT Assay

The SCF extract and spent biomass extracts were tested in various cell lines and MTT assays were conducted to determine their cytotoxicity which is highlighted in **Figures 6-8** and **Table 3,** and discussed below.

MDA-MB-231

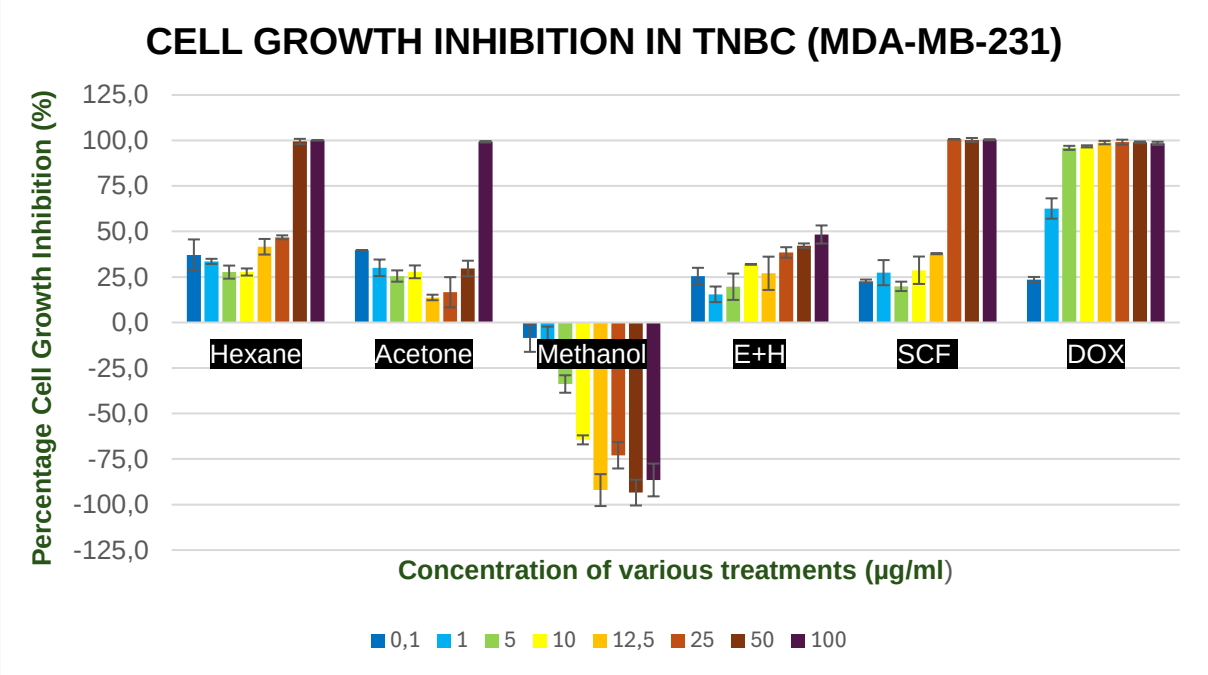

Figure 6: Percentage cell growth inhibition in MDA-MB-231 cells

Figure 6 represents the percentage cell growth inhibition by the five *Cannabis sativa* extracts (hexane, acetone, methanol, E+H and SCF extracts) and the standard breast cancer drug doxorubicin at 0.1 – 100 µg/ml in MDA-MB-231 cell line. All extracts apart

from the methanol extract inhibited the growth of MDA-MB-231 cells and generally, the anti-proliferation potency of the treatments increased as their concentrations increased. This suggests promising anti-cancer effects of *C. sativa* indicating the presence of anti-tumour compounds found in the plant. The effect of methanol extract was an exception as it enhanced MDA-MB-231 cell growth which implies that the extract may lack anti-cancer compounds and/or contains pro-tumour agents. To further determine the efficacy of each treatment, IC_{50} values were calculated and are provided in **Table 5**. Percentage cell growth inhibition values= mean ± standard deviation (SD), n=3. **Legend:** TNBC= triple-negative breast cancer, E+H= ethanol and water, SCF= supercritical carbon dioxide fluid, DOX= doxorubicin.

Vero

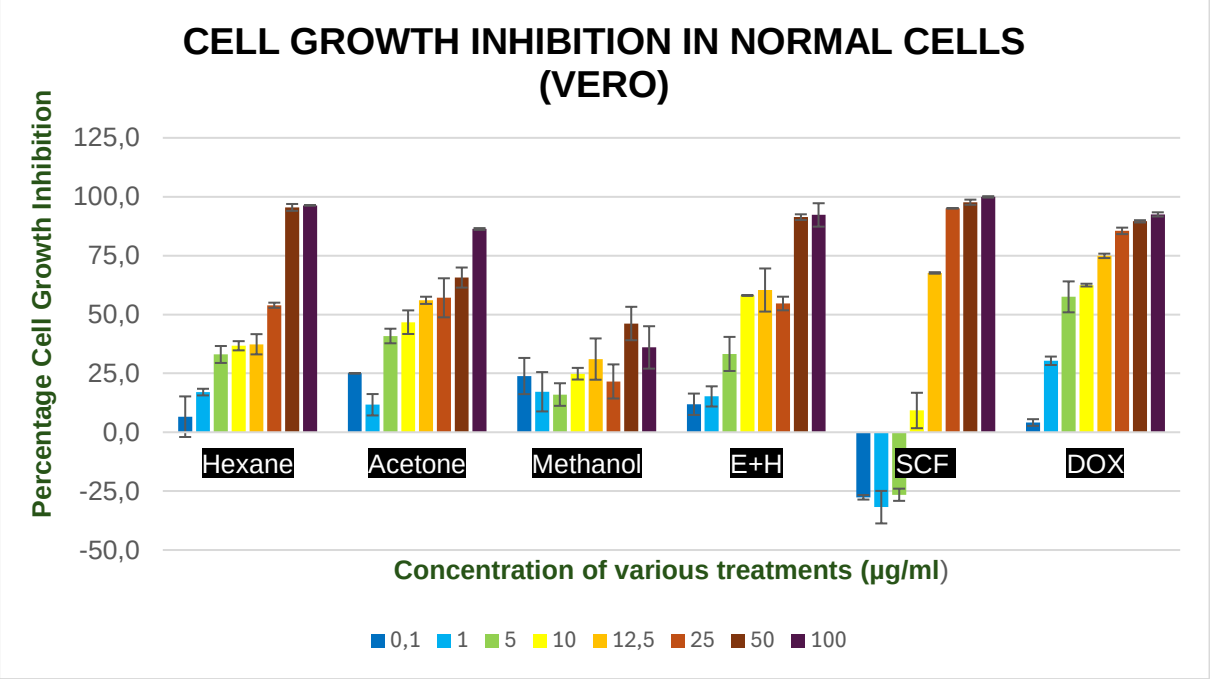

Figure 7: Percentage cell growth inhibition in Vero cells

Figure 7 represents the percentage cell growth inhibition induced by the five *Cannabis sativa* extracts (hexane, acetone, methanol, E+H and SCF extracts) and the standard breast cancer drug doxorubicin at 0.1 – 100 µg/ml in Vero cell line. The MTT assay analysis on normal Vero cells was conducted to assess selective cytotoxicity of the extracts for cancer cells (MDA-MB-231) in comparison to non-cancerous kidney epithelial cells (Vero). All the extracts showed non-selective cytotoxicity as growth inhibition seen in breast cancer cells was also observed with healthy, Vero cells. Generally, the anti-proliferation potency of the treatments increased as their

concentrations increased. However, anti-proliferation remained minimal with methanol extract treatment and at lower concentrations of the SCF extract (0.1 – 10 µg/ml). This suggests that SCF extract may contain a potentially safer combination of anti-cancer compounds compared to the solvent extracts. To further confirm whether the treatments were effective against breast cancer while sparing normal cells, and therefore safe, IC_{50} values provided in **Table 5** were used to calculate the selectivity index (SI) using the formular below:

$$SI = \frac{IC_{50}\ (vero)}{IC_{50}\ (MDA - MB - 231)}$$

Percentage cell growth inhibition values = mean ± SD, n=3. **Legend:** E+H= ethanol and water, SCF= supercritical carbon dioxide fluid, DOX= doxorubicin.

LPS-induced RAW 264.7 macrophages

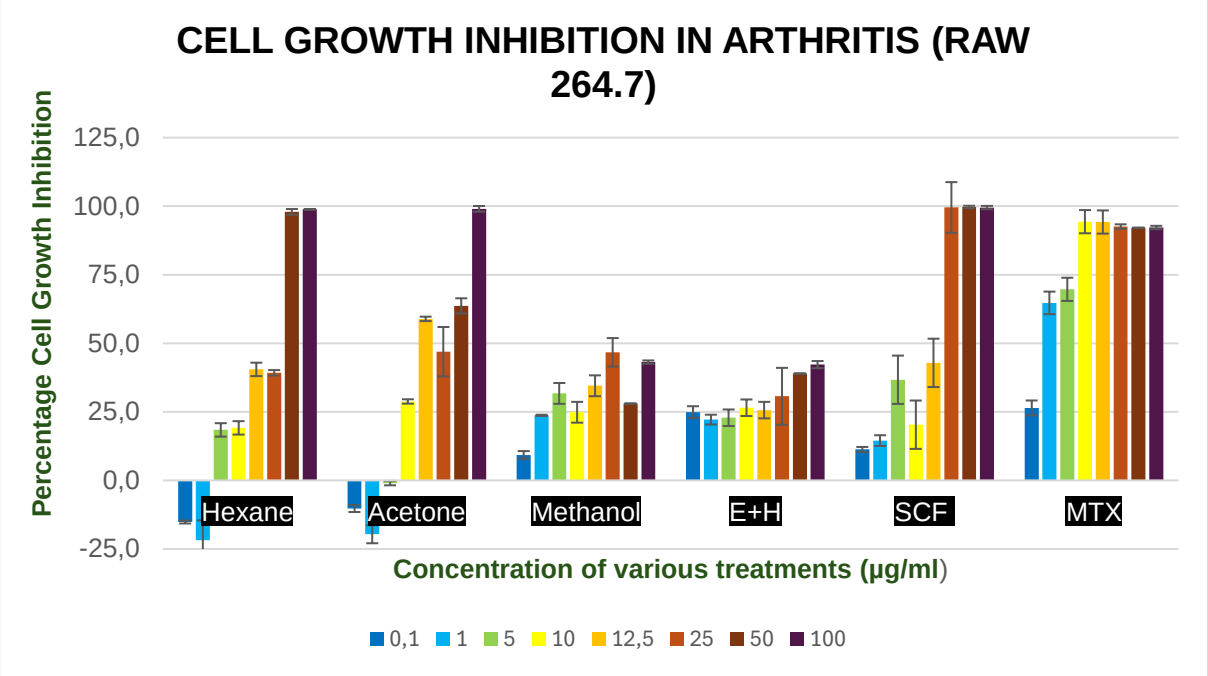

Figure 8: Percentage cell growth inhibition in LPS-stimulated RAW 264.7 macrophages

Figure 8 represents the percentage cell growth inhibition induced by the five *Cannabis sativa* extracts (hexane, acetone, methanol, E+H and SCF extracts) and the standard anti-arthritis drug methotrexate at 0.1 – 100 µg/ml in LPS-induced RAW 264.7 cells. LPS stimulation triggers inflammation in macrophages. Thus, the LPS-stimulated RAW 264.7 macrophages were used as an inflammation model to measure anti-

inflammatory activity. The results illustrate that all the extracts had cytotoxic effects and generally, the anti-proliferation potency of the treatments increased as their concentrations increased. SCF, hexane and acetone extracts had a high cytotoxicity indicating that they contained more bioactive compounds which possess anti-inflammatory activity. However, the low growth inhibition by methanol and E+H extracts and thus lesser suppression of inflammation, suggests a minimal quantity of anti-inflammatory compounds. Percentage cell growth inhibition values= mean ± SD, n=3. **Legend:** E+H= ethanol and water, SCF= supercritical carbon dioxide fluid, MTX= methotrexate.

Table 5: IC_{50} values of the extracts in various cells, as determined by GraphPad Prism version 6, as well as calculated selectivity index values.

Treatment	**MDA-MB-231 (**IC_{50} in µg/ml)	**VERO (**IC_{50} in µg/ml**)**	**SI (Selectivity indices)**	**LPS stimulated RAW 264.7 (**IC_{50} in µg/ml**)**
Hexane	29.7	31.3	1.05	28.8
Acetone	59.9	23.0	0.384	16.7
Methanol	6.40*	-	-	-
E+H	-	-	-	-
SCF	15.1	11.0	0.728	12.8
DOX	5.75	3.29	0.572	N/A
MTX	N/A	N/A	N/A	0.443

Table 5 provides the half maximal inhibitory concentrations (IC_{50}) of individual *Cannabis sativa* extracts and standard drugs tested in the different cell lines. IC_{50} is a measure of effectiveness of a therapeutic agent and the values above indicate the concentrations at which the various extracts and drugs inhibit growth in different cell lines by 50%. Thus, higher IC_{50} means lower potency, while lower IC_{50} means higher potency. The efficacy of extracts tested in this study according to IC_{50} value, ranged from 15.1 – 59.9 µg/ml in MDA-MB-231, 11.0 – 31.3 µg/ml in Vero and 12.8 -28.8 µg/ml

in LPS-stimulated RAW 264.7 macrophages. SCF extract showed the strongest cytotoxic effect against all the cell types as lower concentrations were required for 50% growth inhibition in breast cancer MDA-MB-231 (15.1 µg/ml), healthy Vero (11.0 µg/ml) and inflammatory, LPS-stimulated RAW 264.7 macrophages (12.8 µg/ml). Despite showing significant anti-cancer and anti-inflammatory potential, the high IC_{50} of SCF against Vero cells and low SI value of 0.728 show that it is toxic to both cancer and normal cells, and therefore not safe. The extracts collected using more non-polar solvents also caused notable cytotoxicity in MDA-MB-231. For instance, was the second most potent extract with IC_{50} of 29.7 µg/ml. However, no IC_{50} value could be generated for the E+H and methanol treatment due to percentage inhibition remaining at less than 50% for all tested concentrations of E+H extract and methanol extract inducing cell growth shown by 6.40 µg/ml EC_{50}. **Legend**: IC_{50}= Half Maximal Inhibitory Concentration, *= EC_{50} (Half Maximal Effective Concentration, that is, the concentration at which cell growth is stimulated by 50%), SI= selectivity index where SI value > 3 indicates high selectivity (Prayong *et al.*, 2008), LPS= lipopolysaccharide, E+H= ethanol and water, SCF= supercritical carbon dioxide fluid, DOX= doxorubicin, MTX= methotrexate, - = no value generated, N/A= Positive control does not apply.

According to the MTT assay results given in **Figures 6 -8 and Table 5**, the SCF extract demonstrated the most potent cytotoxicity, with IC_{50} of 15.1 µg/ml in MDA-MB-231, 12.8 µg/ml in the LPS-stimulated RAW 264.7 macrophages and 11.0 µg/ml in vero cells. This suggests that efficacy can be retained in multiple cell types. In the MDA-MB-231 cell line, the results illustrated in **Figure 6** show that considerable cytotoxicity was also induced by the least polar extracts such as hexane which had an IC_{50} of 29.7 µg/ml). However, the E+H treatment showed low levels of cell growth inhibition that fall below 50% for all concentrations. Hence, no IC_{50} value was obtained for the E+H extract. On the other hand, methanol promoted cell growth with an EC_{50} (half-maximal effective concentration) of 6.40 µg/ml. While IC_{50} denotes a concentration at which cell growth inhibition of 50% is reached, EC_{50} describes the concentration at which cell growth is stimulated by 50%.

A study in which different breast cancer cell lines were treated with individual cannabinoids (natural and synthetic CBD as well as novel CBDB and CBDP) showed

efficacy in MDA-MB-231 with IC_{50} values ranging between ~45.3 - 49.3 µM, that is, 14.2 – 16.9 µg/ml (Salbini *et al.*, 2021). The SCF extract in the current study had an IC_{50} of 15.1 µg/ml against MDA-MB-231 cells, that lies within the same range. Moreover, the SCF extract comprised a relatively higher quantity of CBD than the other extracts, which may explain why it also demonstrated greater potency in decreasing breast cancer cell growth. In other TNBC models- SUM159 and 4T1.2, although IC_{50} values were not provided, viability reduced to less than 50% at a lower concentration of 15 µM (~4.72 µg/ml) CBD only treatment (Elbaz *et al.*, 2015). The efficacy of CBD was further validated *in-vivo* by reduced tumor growth and tumor-associated macrophage recruitment following administration (10 mg/kg) in MVT1-1 mice models (Elbaz *et al.*, 2015).

Both findings in combination with the SCF results in this study, suggest that single compounds, particularly CBD, generally show more anti-cancer activity than combinations. However, regarding Elbaz and colleagues, the use of only mouse models *in-vivo* and the disparity of results in different cell lines, most of which were mouse-derived, indicates that using a wider range of human-derived normal and TNBC models, may be more useful in developing treatment suitable for humans.

As demonstrated in **Figure 7**, treatment of the Vero cell line revealed that all the extracts, including E+H and methanol were highly toxic against normal cells. Hence, there is a need to explore ways to enhance specificity of the extracts. A similar study comparing the efficacy of various SCF and solid-liquid *Cannabis sativa* extracts also reported greater efficacy of SCF against MCF-7 (IC_{50}= 13.0-18.0 µg/ml) breast cancer (Pino *et al.*, 2023). However, contrary to this study, both types of extracts showed diminished cytotoxicity in normal MCF-10 breast tissue (SCF IC_{50}= 35.7 - 70.3 µg/ml, solid-liquid extracts IC_{50}= 30.9 - 61.8 µg/ml) (Pino *et al.*, 2023).

With reference to **Figure 8**, in the LPS-stimulated RAW 264.7 macrophages model of inflammation for TNBC and arthritis, the extracts had similar anti-proliferation activity as with MDA-MB-231 cells. However, acetone was more effective than hexane and both induced cell growth at lower concentrations (0.1 - 10 µg/ml) and methanol did not promote proliferation; it only had minimal inhibition effects, similarly to the E+H extract. Fewer *Cannabis sativa* efficacy studies have been conducted on macrophages. In

untreated RAW 264.7 cells, an ethanolic hemp extract and CBD alone were non-cytotoxic at < 125 µg/ml (Kongkadee *et al.*, 2022). However, some bioactivity was observed in other arthritis models. For example, an ethanol *Cannabis sativa* oil extract in macrophage-like, cytokine-secreting WEHI-3 cells, inhibited growth effectively, with IC_{50} of 7.76 ± 0.66 µg/ml after 24 hours (Lteif *et al.*, 2024). Similarly, human RA MH7A synovial cells treated with hempseed oil showed reduced viability at low concentrations, which was found to be caused by ROS accumulation and apoptosis (Jeong *et al.*, 2014).

Lastly, a variety of anti-inflammatory activity assays were conducted to determine the anti-arthritic efficacy of three selected cytotoxic *Cannabis sativa* extracts in RAW 264.7 cells. LPS-induced RAW macrophage IC_{10} values were used to determine which extracts to proceed with in the next anti-inflammatory activity experiments so as to isolate the anti-inflammatory mechanism of action without high cytotoxic levels masking the results. SCF and acetone were selected as the most potent; E+H was chosen due to biocompatibility associated with water-based agents. The results are illustrated in **Tables 6-8** and **Figure 9** and discussed below.

4.3 Nitrite/ Greiss assay

Table 6: Calculated nitrite levels in the different test groups of LPS-stimulated and untreated macrophages

Test/ Control groups	**Post-treatment Nitrite concentration (mM)**
SCF	0.640 ± 0.0671
ACETONE	0.451 ± 0.335
E+H	1.55 ± 0.135
MTX	2.32 ± 0.136
LPS-induced RAW 264.7	4.63 ± 0.658
UNTREATED RAW 264.7 (basal)	2.51 ±0.137

Table 6 outlines nitrite production by LPS-stimulated RAW macrophages under different treatment conditions. Nitrite concentration was quantitatively determined

using the Greiss assay to assess the anti-inflammatory activity of the most potent extracts (SCF and acetone) and water-based E+H at minimal inhibitory (IC_{10}) concentrations (SCF- 10.2 µg/ml, acetone- 8.80 µg/ml, E+H- 23.0 µg/ml) shown in **table A1** under the **appendix**. The nitrite level of ~2.51 mM in the untreated control group represents the basal nitrite production. LPS induction resulted in nitrite upregulation to ~4.63 mM indicating an inflammatory state. Treatment with the extracts was effective in downregulating nitrite synthesis with the acetone extract (~0.451 mM) being the most potent followed by the SCF extract (~0.640 mM). Thus, the extracts demonstrated anti-inflammatory activity. Post-treatment Nitrite concentration values= mean ± SD, n=3. $^{***}P<0.001$ (E+H) and $^{****}P<0.0001$ (SCF and acetone) in **Figure A9** under the Appendix, indicate extremely, statistically significant differences from the LPS-treated group. **Legend**: SCF= supercritical carbon dioxide fluid, E+H= ethanol and water, MTX= methotrexate, LPS= lipopolysaccharide.

According to **Table 6**, the basal nitrite level in non-stimulated, untreated macrophages was 2.51±0.137 mM while LPS stimulation caused an increase to 4.63±0.658 mM. Nitrite production declined to 0.451±0.335, 0.640±0.0671, and 1.55±0.135 mM in acetone, SCF and E+H treated cells, respectively. In comparison, the standard MTX was less effective at reducing LPS stimulation effects by downregulating nitrite concentration to 2.32±0.136 mM. Statistical analysis results in **Figure A9** showed that the most significant difference was visible when comparing LPS-induced RAW 264.7 with SCF and acetone extract treated cells, indicating that both were the most effective at abrogating inflammation.

Nitrite accumulation is an indicator of nitric oxide synthesis by nitric oxide synthase (NOS) in macrophages. nitric oxide is a pro-inflammatory mediator that increases during immune and inflammation responses (Romano *et al.*, 2016). Similar to this study, *Cannabis sativa* extracts and cannabinoids have been reported to inhibit excessive nitric oxide production in LPS-stimulated macrophages. A SCF extract named THCV BDS containing high amounts of ∆9-THCV (64.8%), ∆9-THC (13.5%) and less of CBDV, CBD, CBN, ∆9-THCVA and CBGV, reduced nitric oxide more effectively than THCV alone in murine peritoneal macrophages (Romano *et al.*, 2016). However, Romano and colleagues reported treatment with THCV alone as more potent

despite THCV BDS causing greater declines in nitric oxide levels at low concentrations (0.001-1 µM) and showing a statistically more significant decrease in nitric oxide versus LPS treatment alone at 1 µM. Other experiments assessing THC, CBD, CBC and CBG activity, all of which were found present in the SCF and acetone extracts, have shown their ability to suppress nitric oxide synthesis in macrophages (Romano *et al.*, 2016). Therefore, these cannabinoids likely contributed towards the efficacy of both extracts to reverse nitric oxide accumulation.

4.4 PGE2 ELISA

Table 7: Calculated PGE2 levels in the different test groups of LPS-stimulated and untreated macrophages

Test/ Control groups	**Post-treatment PGE2 concentration (pg/ml)**
SCF	1933 ±87.6
ACETONE	2373 ±94.6
E+H	2614 ±121
MTX	2761 ±62.1
LPS-induced RAW 264.7	3021 ±45.0
UNTREATED RAW 264.7 (basal)	2676 ±150

Table 7 outlines PGE2 production by LPS-stimulated RAW macrophages under different treatment conditions. PGE2 concentration was quantitatively determined using the ELISA to assess the anti-inflammatory activity of the most potent extracts (SCF and acetone) and water-based E+H at minimal inhibitory (IC_{10}) concentrations (SCF- 10.2 µg/ml, acetone- 8.80 µg/ml, E+H- 23.0 µg/ml). The PGE2 concentration of ~2676 pg/ml in the untreated control group represents basal PGE2 synthesis in the macrophages. LPS induction resulted in increased levels of PGE2 to ~3021 pg/ml indicating a state of inflammation. Treatment with the extracts effectively inhibited PGE2 synthesis such that the SCF extract (~1933 pg/ml) was most potent followed by the acetone extract (~2373 pg/ml). This further highlighted the anti-inflammatory properties possessed by *C. sativa.* Post-treatment PGE2 concentration values= mean ± SD, n=3. $^{**}P<0.01$ (E+H), $^{***}P<0.001$ (acetone) and $^{****}P<0.0001$ (SCF) in **Figure A11** under the Appendix, indicate highly to extremely, statistically significant

differences from the LPS-treated group. Legend: PGE2= Prostaglandin E_2, SCF= supercritical carbon dioxide fluid, E+H= ethanol and water, MTX= methotrexate, LPS= lipopolysaccharide**.**

The results in **Table 7** also show that the extracts downregulated PGE2 synthesis from 3021±45.0 pg/ml to as low as 1933±87.6 pg/ml in SCF extract treated cells compared to 2761±62.1 pg/ml by MTX. Furthermore, the BCA assay results presented in **Table 8**, demonstrated a lower amount of protein in SCF extract (277±15.6 µg/ml) and acetone extract (251±36.1 µg/ml) treated samples versus the LPS-induced sample (320±8.56 µg/ml), suggesting that the synthesis of certain proteins was suppressed by the extracts and positive control MTX (249±6.40 µg/ml). However, higher protein content was quantified in the E+H extract (348±0.0956 µg/ml). Statistical analysis revealed that SCF was significantly more potent for PGE2 inhibition than all treatments, followed by acetone, which was notably more effective compared to MTX and LPS alone. Basal PGE2 levels were also markedly lower than in LPS-induced macrophages.

4.5 BCA Assay

Table 8: Calculated protein levels in the different test groups of LPS-stimulated and untreated macrophages

Test/ Control groups	**protein concentration (µg/ml)**
SCF	277 ±15.6
ACETONE	251 ±36.1
E+H	348 ±0.0956
MTX	249 ±6.40
LPS-induced RAW 264.7	320 ±8.56
UNTREATED RAW 264.7 (basal)	178 ±19.5

Table 8 outlines protein synthesis by LPS-stimulated RAW macrophages under different treatment conditions. Protein concentration was quantitatively determined

using the BCA assay to assess the anti-inflammatory activity of the most potent extracts (SCF and acetone) and water-based E+H at minimal inhibitory (IC_{10}) concentrations (SCF- 10.2 µg/ml, acetone- 8.80 µg/ml, E+H- 23.0 µg/ml). Post-treatment protein concentration values= mean ± SD, n=3. *P*>0.05 (SCF and E+H) and **P*<0.05 (acetone) in **Figure A13** under the Appendix, indicate none and a statistically significant difference, respectively, from the LPS-treated group. **Legend:** SCF= supercritical carbon dioxide fluid, E+H= ethanol and water, MTX= methotrexate, LPS= lipopolysaccharide.

4.6 Coomasie-blue staining

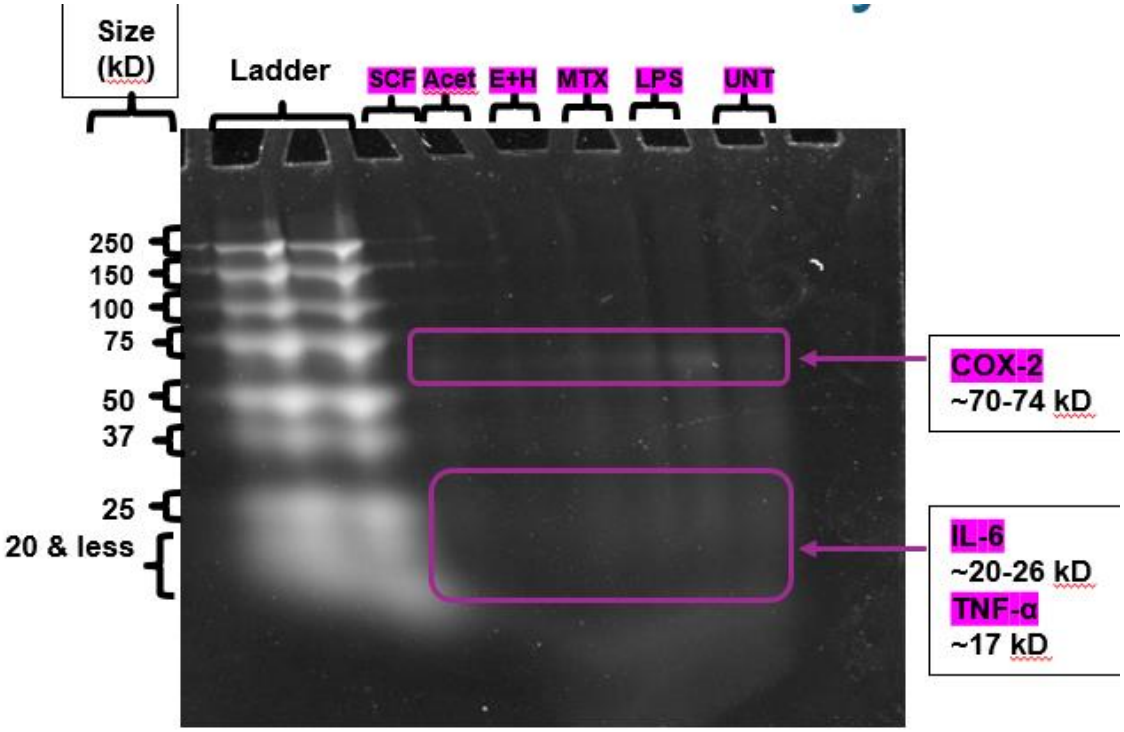

Figure 9: Qualitative Coomassie-blue staining results

Figure 9 displays the qualitative analysis results of IL-6, TNF-α and COX-2 protein expression for varying treatment conditions as determined utilizing Coomasie-blue staining. This was a preliminary test conducted prior to western blotting to observe the potential effects of the most potent extracts (SCF and acetone) and water-based E+H at minimal inhibitory (IC_{10}) concentrations (SCF- 10.2 µg/ml, acetone- 8.80 µg/ml, E+H-

23.0 µg/ml), on the expression of common inflammatory biomarkers in LPS-stimulated macrophages. **Legend:** SCF= supercritical carbon dioxide fluid, Acet= acetone, E+H= ethanol and water, MTX= methotrexate, LPS= lipopolysaccharide, UNT= untreated, kD= Kilodalton, COX-2= Cyclooxygenase-2, IL-6= Interleukin-6, TNF-α= Tumor Necrosis Factor Alpha.

LPS-induction was confirmed to be successful as the protein biomarker levels were most elevated in LPS-stimulated only macrophages. Furthermore, the tested extracts were found to be effective in reducing the LPS-induced protein upregulation. Although COX-2 antibody probing was unsuccessful in the Western blot experiment, coomassie-blue staining results in **Figure 9,** illustrated distinct bands across all samples of protein sizes between 50-75 kD and equal to or slightly more than 25 kD, where COX-2 weighing 70-74 kD, IL-6 (20-26 kD) and TNF-α (17 kD) fall. The preliminary results in **Figure 9** showed that the band intensity correlating to protein expression levels faded towards the left where the extract samples lie, while the greatest intensity was visible in the LPS protein sample. The results further indicated the successful induction of inflammation by LPS and suggest that this was significantly reversed by treatment with extracts more effectively than MTX.

Previous studies have shown *Cannabis sativa* anti-arthritic role in moderating inflammation biomarkers. For instance, IL-1β-induced synovial fibroblasts (SW982) treated with methanolic hemp seed extracts responded with reduced nitric oxide, PGE2 and gene expression of the synthases responsible for their production (iNOS, COX-2) (Duangnin *et al.*, 2017). More than one concentration was tested and similarly to this study, the extracts were more effective than the standard drug used (dexamethasone) (Duangnin *et al.*, 2017). Also, the extract of the cultivar with the highest amount of THC showed the most potency (Duangnin *et al.*, 2017). Likewise, THCV alone attenuated COX-2 expression in murine peritoneal macrophages (Romano *et al.*, 2016). On the contrary, CBD increased IL-6 and TNF-α levels in RAW 264.7 macrophages, illustrating pro-inflammatory action (Muthumalage and Rahman, 2019). This may be counteracted by other phytochemicals found in *Cannabis sativa* extracts, since these demonstrated opposite activity. Similarly, CBD was less effective compared to a cocktail comprising CBD and moringa (5 µM each), which increased their individual efficacy of suppression

of cytokine secretion in LPS-stimulated macrophages (Rajan *et al.*, 2016). Down-regulated pro-inflammatory markers included TNF-α and iNOS (Rajan *et al.*, 2016).

CHAPTER 6: CONCLUSION

From this study, it was concluded that SCF extraction allows for significant extraction of bioactive and potent phytochemicals from *Cannabis sativa* plant material; however, the waste biomass material still retains therapeutic potential. This is illustrated by SCF, hexane and acetone extracts, which contained the highest cannabinoid content, also being the most effective at inhibiting TNBC (MDA-MB-231) and LPS-induced RAW 264.7 (found in both breast cancer and arthritis inflammatory microenvironments) cell growth. Further highlighting their efficacy is the ability to reverse overexpression of inflammatory mediators (nitrites, PGE2 and potentially IL-6, TNF-α and COX-2) and the fact that they performed better than the MTX golden standard. These observations emphasize the potential anticancer and anti-inflammatory efficacy of *C. sativa* and demonstrate that this can be attributed to the notable presence of phytochemicals such as cannabinoids.

Study limitations

- Use of few *in-vitro* models, some of which are not human-derived (monkey vero and murine RAW 264.7 macrophages) may provide a limited view of the effects of the *Cannabis sativa* extracts in human hosts.
- Some of the MTT assay results showed fluctuation of cytotoxicity with increasing concentration of treatment and thus generated inconsistent IC_{50} values.
- In the Western blot experiment, the minimal transfer of the protein onto membrane and weak binding of COX-2 antibodies may be due to insufficient protein extraction.
- A lack of cannabinoid standards and primary antibodies for IL-6 and TNF-α due to limited funds limited an extensive investigation of the therapeutic potential of *Cannabis sativa* extract using the LC-MS and western blot techniques.

Future studies

- It is necessary to explore targeted delivery methods, such as nanoencapsulation, to enhance specificity and the therapeutic potential of the *Cannabis sativa* extracts.
- Another avenue worth exploring to improve efficacy is combining *Cannabis*

sativa-derived substances with other medicinal products.

- It is recommended that LC-MS be repeated with analyte standards or at least one reference standard for a selected phytochemical should be used in future to properly quantify that phytochemical as a representative or surrogate for the extract. While western blot should be performed with other inflammatory mediator antibodies to further validate the results obtained in this study.
- Co-culture experiments are recommended to simulate the tumour microenvironment. For instance, extract treatments may be introduced into a culture made up of both TNBC cell lines and RAW 264.7 macrophages. Animal studies may then follow to assess *in-vivo* effects.
- In future, the concentration of solvent in each extract will be analysed to ensure that there is minimal solvent cytotoxicity affecting MTT assay results.
- To confirm identification of COX-2, IL-6 and TNF-alpha, ELISA assays may be employed in future.

References

Aizpurua-Olaizola, O. *et al.* (2014) 'Identification and quantification of cannabinoids in Cannabis sativa L. plants by high performance liquid chromatography-mass spectrometry', *Analytical and Bioanalytical Chemistry*, 406(29), pp. 7549–7560. Available at: https://doi.org/10.1007/s00216-014-8177-x.

Allegrone, G. *et al.* (2017) 'The Bibenzyl Canniprene Inhibits the Production of Pro-Inflammatory Eicosanoids and Selectively Accumulates in Some Cannabis sativa Strains', *Journal of Natural Products*, 80(3), pp. 731–734. Available at: https://doi.org/10.1021/acs.jnatprod.6b01126.

Bala, A. *et al.* (2019) 'UPLC-MS Analysis of *Cannabis sativa* Using Tetrahydrocannabinol (THC), Cannabidiol (CBD), and Tetrahydrocannabinolic Acid (THCA) as Marker Compounds: Inhibition of Breast Cancer Cell Survival and Progression', *Natural Product Communications*, 14(8), pp. 1–5. Available at: https://doi.org/10.1177/1934578X19872907.

Balant, M. *et al.* (2021) 'Traditional uses of Cannabis: An analysis of the CANNUSE database', *Journal of Ethnopharmacology*, 279, p. 114362. Available at: https://doi.org/10.1016/j.jep.2021.114362.

Berger, M.F. and Mardis, E.R. (2018) 'The emerging clinical relevance of genomics in cancer medicine', *Nature reviews. Clinical oncology*, 15(6), pp. 353–365. Available at: https://doi.org/10.1038/s41571-018-0002-6.

Blasco-Benito, S. *et al.* (2018) 'Appraising the "entourage effect": Antitumor action of a pure cannabinoid versus a botanical drug preparation in preclinical models of breast cancer', *Biochemical Pharmacology*, 157, pp. 285–293. Available at: https://doi.org/10.1016/j.bcp.2018.06.025.

Booth, J.K. and Bohlmann, J. (2019) 'Terpenes in Cannabis sativa – From plant genome to humans', *Plant Science*, 284, pp. 67–72. Available at: https://doi.org/10.1016/j.plantsci.2019.03.022.

Chang, M.H. and Nigrovic, P.A. (2019) 'Antibody-dependent and -independent mechanisms of inflammatory arthritis', *JCI Insight*, 4(5), p. e125278. Available at: https://doi.org/10.1172/jci.insight.125278.

Cheng, C.-F., Liao, H.-J. and Wu, C.-S. (2022) 'Tissue microenvironment dictates inflammation and disease activity in rheumatoid arthritis', *Journal of the Formosan Medical Association*, 121(6), pp. 1027–1033. Available at: https://doi.org/10.1016/j.jfma.2022.01.026.

Citti, C. *et al.* (2018) 'A Metabolomic Approach Applied to a Liquid Chromatography Coupled to High-Resolution Tandem Mass Spectrometry Method (HPLC-ESI-HRMS/MS): Towards the Comprehensive Evaluation of the Chemical Composition of Cannabis Medicinal Extracts', *Phytochemical Analysis*, 29(2), pp. 144–155. Available at: https://doi.org/10.1002/pca.2722.

Citti, C. *et al.* (2019) 'Cannabinoid Profiling of Hemp Seed Oil by Liquid Chromatography Coupled to High-Resolution Mass Spectrometry', *Frontiers in Plant*

Science, 10, p. 120. Available at: https://doi.org/10.3389/fpls.2019.00120.

da Costa Vieira, R.A. *et al.* (2017) 'Breast cancer screening in developing countries', *Clinics*, 72(4), pp. 244–253. Available at: https://doi.org/10.6061/clinics/2017(04)09.

Danforth, D.N. (2021) 'The Role of Chronic Inflammation in the Development of Breast Cancer', *Cancers*, 13(15), p. 3918. Available at: https://doi.org/10.3390/cancers13153918.

Di Giacomo, S. *et al.* (2021) 'Role of Caryophyllane Sesquiterpenes in the Entourage Effect of Felina 32 Hemp Inflorescence Phytocomplex in Triple Negative MDA-MB-468 Breast Cancer Cells', *Molecules (Basel, Switzerland)*, 26(21), p. 6688. Available at: https://doi.org/10.3390/molecules26216688.

Duangnin, N. *et al.* (2017) 'Anti-inflammatory effect of methanol extracts of hemp leaf in IL-1β-induced synovitis', *Tropical Journal of Pharmaceutical Research*, 16(7), pp. 1553–1563. Available at: https://doi.org/10.4314/tjpr.v16i7.13.

Dudics, S. *et al.* (2018) 'Natural Products for the Treatment of Autoimmune Arthritis: Their Mechanisms of Action, Targeted Delivery, and Interplay with the Host Microbiome', *International Journal of Molecular Sciences*, 19(9), p. 2508. Available at: https://doi.org/10.3390/ijms19092508.

Elbaz, M. *et al.* (2015) 'Modulation of the tumor microenvironment and inhibition of EGF/EGFR pathway: novel anti-tumor mechanisms of Cannabidiol in breast cancer', *Molecular oncology*, *9*(4), 906–919. https://doi.org/10.1016/j.molonc.2014.12.010

Elbaz, M. *et al.* (2017) 'Novel role of cannabinoid receptor 2 in inhibiting EGF/EGFR and IGF-I/IGF-IR pathways in breast cancer', *Oncotarget*, 8(18), pp. 29668–29678. Available at: https://doi.org/10.18632/oncotarget.9408.

Farinon, B. *et al.* (2020) 'The Seed of Industrial Hemp (Cannabis sativa L.): Nutritional Quality and Potential Functionality for Human Health and Nutrition', *Nutrients*, 12(7), p. 1935. Available at: https://doi.org/10.3390/nu12071935.

George KL. *et al.* (2008) 'Ajulemic acid, a nonpsychoactive cannabinoid acid, suppresses osteoclastogenesis in mononuclear precursor cells and induces apoptosis in mature osteoclast-like cells', *J Cell Physiol.* 214(3): pp. 714-20. Available at: doi: 10.1002/jcp.21263. PMID: 17786950.

Gui H. *et al.* (2014) 'Activation of cannabinoid receptor 2 attenuates synovitis and joint distruction in collagen-induced arthritis', *Immunobiology.* 220(6): pp.817-22. Available at: doi: 10.1016/j.imbio.2014.12.012. PMID: 25601571.

Hirao-Suzuki, M. *et al.* (2020) 'Cannabidiolic acid dampens the expression of cyclooxygenase-2 in MDA-MB-231 breast cancer cells: Possible implication of the peroxisome proliferator-activated receptor β/δ abrogation', *The Journal of Toxicological Sciences*, 45(4), pp. 227–236. Available at: https://doi.org/10.2131/jts.45.227.

Jeong, M. *et al.* (2014) ‘Hempseed oil induces reactive oxygen species- and C/EBP homologous protein-mediated apoptosis in MH7A human rheumatoid arthritis fibroblast-like synovial cells’, *Journal of Ethnopharmacology*, 154(3), pp. 745–752. Available at: https://doi.org/10.1016/j.jep.2014.04.052.

Kisková, T. *et al.* (2019) ‘Future Aspects for Cannabinoids in Breast Cancer Therapy’, *International Journal of Molecular Sciences*, 20(7), p. 1673. Available at: https://doi.org/10.3390/ijms20071673.

Kongkadee, K. *et al.* (2022) ‘Anti-inflammation and gingival wound healing activities of *Cannabis sativa* L. subsp. *sativa* (hemp) extract and cannabidiol: An *in vitro* study’, *Archives of Oral Biology*, 140, p. 105464. Available at: https://doi.org/10.1016/j.archoralbio.2022.105464.

Kundu, J.K. and Surh, Y.-J. (2012) ‘Emerging avenues linking inflammation and cancer’, *Free Radical Biology and Medicine*, 52(9), pp. 2013–2037. Available at: https://doi.org/10.1016/j.freeradbiomed.2012.02.035.

Lal, S. *et al.* (2021) ‘Cannabis and its constituents for cancer: History, biogenesis, chemistry and pharmacological activities’, *Pharmacological Research*, 163, p. 105302. Available at: https://doi.org/10.1016/j.phrs.2020.105302.

Legare, C.A., Raup-Konsavage, W.M. and Vrana, K.E. (2022) ‘Therapeutic Potential of Cannabis, Cannabidiol, and Cannabinoid-Based Pharmaceuticals’, *Pharmacology*, 107(3–4), pp. 131–149. Available at: https://doi.org/10.1159/000521683.

Laragione T, Cheng KF, Tanner MR, He M, Beeton C, Al-Abed Y, Gulko PS. 2015 'The cation channel Trpv2 is a new suppressor of arthritis severity, joint damage, and synovial fibroblast invasion', *Clin Immunol.* 158(2): pp. 183-92. doi: 10.1016/j.clim.2015.04.001. PMID: 25869297; PMCID: PMC4617367

Lehmann, B.D. *et al.* (2011) ‘Identification of human triple-negative breast cancer subtypes and preclinical models for selection of targeted therapies’, *The Journal of Clinical Investigation*, 121(7), pp. 2750–2767. Available at: https://doi.org/10.1172/JCI45014.

Lin, Y.-J., Anzaghe, M. and Schülke, S. (2020) ‘Update on the Pathomechanism, Diagnosis, and Treatment Options for Rheumatoid Arthritis’, *Cells*, 9(4), p. 880. Available at: https://doi.org/10.3390/cells9040880.

Lowin, T. *et al.* (2020) ‘Cannabidiol (CBD): a killer for inflammatory rheumatoid arthritis synovial fibroblasts’, *Cell Death & Disease*, 11(8), p. 714. Available at: https://doi.org/10.1038/s41419-020-02892-1.

Lteif, A. *et al.* (2024) ‘Lebanese cannabis oil as a potential treatment for acute myeloid leukemia: *In vitro* and *in vivo* evaluations’, *Journal of Ethnopharmacology*, 333, p. 118512. Available at: https://doi.org/10.1016/j.jep.2024.118512.

Lukhele, S.T. and Motadi, L.R. (2016) ‘Cannabidiol rather than Cannabis sativa extracts inhibit cell growth and induce apoptosis in cervical cancer cells’, *BMC Complementary and Alternative Medicine*, 16(1), p. 335. Available at: https://doi.org/10.1186/s12906-016-1280-0.

Malfait AM. *et al.* (2000) 'The nonpsychoactive cannabis constituent cannabidiol is an oral anti-arthritic therapeutic in murine collagen-induced arthritis'. *Proc Natl Acad Sci U S A.* 97(17): pp. 9561-6. doi: 10.1073/pnas.160105897. PMID: 10920191; PMCID: PMC16904.

Mariani, F.M. *et al.* (2023) 'Pathogenesis of rheumatoid arthritis: one year in review 2023', *Clinical and Experimental Rheumatology*, 41(9), pp. 1725–1734. Available at: https://doi.org/10.55563/clinexprheumatol/sgjk6e.

Mbvundula EC, Bunning RA, Rainsford KD (2006) 'Arthritis and cannabinoids: HU-210 and Win-55,212-2 prevent IL-1alpha-induced matrix degradation in bovine articular chondrocytes *in-vitro*', *J Pharm Pharmacol.,* 58(3): pp351-8. doi: 10.1211/jpp.58.3.0009. PMID: 16536902.

McAllister, S.D. *et al.* (2007) 'Cannabidiol as a novel inhibitor of Id-1 gene expression in aggressive breast cancer cells', *Molecular Cancer Therapeutics*, 6(11), pp. 2921–2927. Available at: https://doi.org/10.1158/1535-7163.MCT-07-0371.

McInnes, I.B. and Schett, G. (2017) 'Pathogenetic insights from the treatment of rheumatoid arthritis', *The Lancet*, 389(10086), pp. 2328–2337. Available at: https://doi.org/10.1016/S0140-6736(17)31472-1.

Mcrae, G. and Melanson, J. (2020) 'Quantitative determination and validation of 17 cannabinoids in cannabis and hemp using liquid chromatography-tandem mass spectrometry', *Analytical and Bioanalytical Chemistry*, 412. Available at: https://doi.org/10.1007/s00216-020-02862-8.

McRae, G. and Melanson, J.E. (2020) 'Quantitative determination and validation of 17 cannabinoids in cannabis and hemp using liquid chromatography-tandem mass spectrometry', *Analytical and Bioanalytical Chemistry*, 412(27), p. 7381. Available at: https://doi.org/10.1007/s00216-020-02862-8.

Meng, Q. *et al.* (2018) 'A reliable and validated LC-MS/MS method for the simultaneous quantification of 4 cannabinoids in 40 consumer products', *PloS One*, 13(5), p. e0196396. Available at: https://doi.org/10.1371/journal.pone.0196396.

Muthumalage, T. and Rahman, I. (2019) 'Cannabidiol differentially regulates basal and LPS-induced inflammatory responses in macrophages, lung epithelial cells, and fibroblasts', *Toxicology and Applied Pharmacology*, 382, p. 114713. Available at: https://doi.org/10.1016/j.taap.2019.114713.

Nagarkatti, P. *et al.* (2009) 'Cannabinoids as novel anti-inflammatory drugs', *Future medicinal chemistry*, 1(7), pp. 1333–1349. Available at: https://doi.org/10.4155/fmc.09.93.

NCI (2021) *What Is Cancer?* Available at: https://www.cancer.gov/about-cancer/understanding/what-is-cancer (Accessed: 23 May 2022).

Pantoja-Ruiz, C. *et al.* (2021) 'Cannabis and pain: a scoping review', *Brazilian Journal of Anesthesiology*, 72(1), p. 142. Available at: https://doi.org/10.1016/j.bjane.2021.06.018.

Pellati, F. *et al.* (2018) ‘Cannabis sativa L. and Nonpsychoactive Cannabinoids: Their Chemistry and Role against Oxidative Stress, Inflammation, and Cancer’, *BioMed Research International*, 2018, p. 1691428. Available at: https://doi.org/10.1155/2018/1691428.

Pino, S. *et al.* (2023) ‘Study of Cannabis Oils Obtained from Three Varieties of C. sativa and by Two Different Extraction Methods: Phytochemical Characterization and Biological Activities’, *Plants*, 12(9), p. 1772. Available at: https://doi.org/10.3390/plants12091772.

Pol, J. *et al.* (2022) ‘Beneficial autoimmunity and maladaptive inflammation shape epidemiological links between cancer and immune-inflammatory diseases’, *OncoImmunology*, 11(1), p. 2029299. Available at: https://doi.org/10.1080/2162402X.2022.2029299.

Poudel, P., Goyal, A. and Lappin, S.L. (2022) ‘Inflammatory Arthritis’, in *StatPearls [Internet]*. StatPearls Publishing. Available at: https://www.ncbi.nlm.nih.gov/books/NBK507704/ (Accessed: 25 May 2023).

Prayong P, Barusrux S, Weerapreeyakul N. (2008) 'Cytotoxic activity screening of some indigenous Thai plants', *Fitoterapia*, 79(7-8), pp. 598-601. doi: 10.1016/j.fitote.2008.06.007. Epub 2008 Jul 11. PMID: 18664377.

Rajan, T.S. *et al.* (2016) ‘Anti-inflammatory and antioxidant effects of a combination of cannabidiol and moringin in LPS-stimulated macrophages’, *Fitoterapia*, 112, pp. 104–115. Available at: https://doi.org/10.1016/j.fitote.2016.05.008.

Rodríguez Mesa, X.M. *et al.* (2021) ‘Therapeutic Prospects of Cannabinoids in the Immunomodulation of Prevalent Autoimmune Diseases’, *Cannabis and Cannabinoid Research*, 6(3), pp. 196–210. Available at: https://doi.org/10.1089/can.2020.0183.

Romano, B. *et al.* (2016) ‘Pure Δ 9 -tetrahydrocannabivarin and a Cannabis sativa extract with high content in Δ 9 -tetrahydrocannabivarin inhibit nitrite production in murine peritoneal macrophages’, *Pharmacological Research*, 113, pp. 199–208. Available at: https://doi.org/10.1016/j.phrs.2016.07.045.

Salbini, M. *et al.* (2021) ‘Oxidative Stress and Multi-Organel Damage Induced by Two Novel Phytocannabinoids, CBDB and CBDP, in Breast Cancer Cells’, *Molecules*, 26(18), p. 5576. Available at: https://doi.org/10.3390/molecules26185576.

Sarzi-Puttini, P. *et al.* (2024) ‘“Inflammatory or non-inflammatory pain in inflammatory arthritis – How to differentiate it?”’, *Best Practice & Research Clinical Rheumatology*, 38(1), p. 101970. Available at: https://doi.org/10.1016/j.berh.2024.101970.

Schoeman, R. *et al.* (2022) ‘Cannabis with breast cancer treatment: propitious or pernicious?’, *3 Biotech*, 12(2), p. 54. Available at: https://doi.org/10.1007/s13205-021-03102-1.

Selvi E. *et al.* (2008) 'Inhibitory effect of synthetic cannabinoids on cytokine production in rheumatoid fibroblast-like synoviocytes', *Clin Exp Rheumatol,* 26(4): pp 574-81. PMID: 18799087.

Shrivastava, A. *et al.* (2011) 'Cannabidiol Induces Programmed Cell Death in Breast Cancer Cells by Coordinating the Cross-talk between Apoptosis and Autophagy', *Molecular Cancer Therapeutics*, 10(7), pp. 1161–1172. Available at: https://doi.org/10.1158/1535-7163.MCT-10-1100.

Singh, N. *et al.* (2019) 'Inflammation and Cancer', *Annals of African Medicine*, 18(3), pp. 121–126. Available at: https://doi.org/10.4103/aam.aam_56_18.

Sukumar, J. *et al.* (2021) 'Triple-negative breast cancer: promising prognostic biomarkers currently in development', *Expert review of anticancer therapy*, 21(2), pp. 135–148. Available at: https://doi.org/10.1080/14737140.2021.1840984.

Sumariwalla PF. *et al.* (2004) 'A novel synthetic, nonpsychoactive cannabinoid acid (HU-320) with antiinflammatory properties in murine collagen-induced arthritis', *Arthritis Rheum.,* 50(3): pp 985-98. doi: 10.1002/art.20050. PMID: 15022343.

Tavčar Kunstič, T., Debeljak, N. and Fon Tacer, K. (2023) 'Heterogeneity in hormone-dependent breast cancer and therapy: Steroid hormones, HER2, melanoma antigens, and cannabinoid receptors', *Advances in Cancer Biology - Metastasis*, 7, p. 100086. Available at: https://doi.org/10.1016/j.adcanc.2022.100086.

Ubeed, H.M.S.A. *et al.* (2022) 'A Comprehensive Review on the Techniques for Extraction of Bioactive Compounds from Medicinal Cannabis', *Molecules*, 27(3), p. 604. Available at: https://doi.org/10.3390/molecules27030604.

Usenbo, A. *et al.* (2015) 'Prevalence of Arthritis in Africa: A Systematic Review and Meta-Analysis', *PLoS ONE*, 10(8), p. e0133858. Available at: https://doi.org/10.1371/journal.pone.0133858.

Villarreal-García, V. *et al.* (2022) 'A vicious circle in breast cancer: The interplay between inflammation, reactive oxygen species, and microRNAs', *Frontiers in Oncology*, 12. Available at: https://doi.org/10.3389/fonc.2022.980694.

Waks, A.G. and Winer, E.P. (2019) 'Breast Cancer Treatment: A Review', *JAMA*, 321(3), pp. 288–300. Available at: https://doi.org/10.1001/jama.2018.19323.

WHO (2024) *Breast cancer*, *World Health Organisation*. Available at: https://www.who.int/news-room/fact-sheets/detail/breast-cancer (Accessed: 1 December 2024).

Won, H.S. *et al.* (2022) 'Clinical significance of HER2-low expression in early breast cancer: a nationwide study from the Korean Breast Cancer Society', *Breast Cancer Research*, 24(1), p. 22. Available at: https://doi.org/10.1186/s13058-022-01519-x.

Yin, L. *et al.* (2020) 'Triple-negative breast cancer molecular subtyping and treatment progress', *Breast Cancer Research : BCR*, 22, p. 61. Available at: https://doi.org/10.1186/s13058-020-01296-5.

Zagzoog, A. *et al.* (2020) '*In vitro* and *in vivo* pharmacological activity of minor

cannabinoids isolated from Cannabis sativa', *Scientific Reports*, 10(1), p. 20405. Available at: https://doi.org/10.1038/s41598-020-77175-y.

Zirpel, B., Kayser, O. and Stehle, F. (2018) 'Elucidation of structure-function relationship of THCA and CBDA synthase from *Cannabis sativa* L.', *Journal of Biotechnology*, 284, pp. 17–26. Available at: https://doi.org/10.1016/j.jbiotec.2018.07.031.

Zurier RB, Rossetti RG, Burstein SH, Bidinger B. (2003) 'Suppression of human monocyte interleukin-1beta production by ajulemic acid, a nonpsychoactive cannabinoid', *Biochem Pharmacol,* 65(4): pp. 649-55. doi: 10.1016/s0006-2952(02)01604-0. PMID: 12566094.

Appendix

1. Apparatus

Cannabis sativa collection and extraction

For mixing the plant material with solvent, 2.5 L recycled reagent bottles were used. Weighing boats were used to contain the plant material while weighing on the mass scale (aeADAM, PGL 6001, Max 6000g, d=0.1g). A horizontal shaker (FMH200, FMH Instruments, Stargate Scientific) was used to agitate the mixture. 1000 ml glass bottles (SIMAX, Czech Republic), 1000 ml conical flasks (GLASSCO), funnels (SCHOTT, DURAN), 500 ml measuring cylinder (BTL, South Africa), filter papers (Grade 3hw, 65 g/m^3, 240mm, BOECO, Germany), and paper towels were utilized throughout for the transfer of materials and reagents for extraction, drying, filtration and filtrate concentration in a rotary evaporator (EINS SCI E-RE-V, Stargate Scientific). The collected extracts were further concentrated in glass petri-dishes placed in a fume cupboard (Vivid Air Filtration and Ventilation Suppliers). The Supercritical CO_2 Fluid extraction system (HMI) at the TUT-CSIR hub was used to perform SCF extraction.

LC-MS

Glass test tubes and Eppendorf tubes were used to combine extracts in different solvents (DMSO, methanol and 1 % methanol) to establish solubility and prepare stock solutions using suitable solvents that do not cause sedimentation in the mixtures. Final extract solutions were filtered using 0.45 µm syringe filter. The QTRAP 4500 LC-MS/MS System (SCIEX), Shimadzu Nexera Series (Shimadzu version 1.61) was equipped with a TurbulonSpray ion source. MS acquisition parameters were set as follows: 2.1 E-5 Torr vacuum pressure, curtain gas at 35 psi and both Ion source gas 1 and 2 at 50 psi, 500°C source temperature, MRM scan, positive polarity, 5000 V spray voltage and nitrogen was used as a collision gas. The set up included a Kinetex 2.6 µm C18 100 Å 50 × 2.1 mm column, mobile phase of 0.1% (v/v) formic acid acidified water (solvent A), 0.1% (v/v) formic acid acidified methanol (solvent B), and 1.5 ml VT54 vial plate.

MTT

Materials used include a BIOBASE electronic analytical balance (Biosmart Scientific) for weighing, a Digital Dry Bath incubator for warming reagents intended for use on cells to 37°C, NF 400 Micro High-Speed centrifuge (Nuve, BIOBASE) for obtaining cell pellets, TC20 Automated cell counter (BIORAD) for determining cell count and viability. Cells were contained in sterile T25 and T75 cell culture flasks (SPL Life Sciences) and

seeded in 96 well plates for MTT assays. An inverted Biological microscope (BIOBASE) was used for viewing cell morphology and growth. Working reagents including cell suspensions were transferred into 15 ml and 50 ml Cellstar centrifuge tubes (Greiner Bio-one), eppendorf tubes, and cryovials using autoclavable Nichipet EXII micropipettes (2-20 µl, 20-200 µl and 100-1000 µl), autoclaved micro tips, DLAB Levo Plus pipette gun and sterile serological pipettes. Cell culture experiments were performed under a clean bench ZHJH-1118C laminar flow hood (Micro Filtration) employing an aseptic technique according to laboratory protocol. Cells were kept in the BJPX-C160 CO_2 Incubator (BIOBASE). A Glomax Discover Multimode plate reader (Promega) was used to take absorbance readings for colorimetric assays

Nitrite/ Greiss Assay

Contents of Invitrogen Griess reagent Kit (Thermo Fisher Scientific)- 0.1% (1 mg/mL) N-(1-naphthyl)ethylenediamine dihydrochloride solution (Component A), 1% (10 mg/mL) Sulfanilic acid in 5% phosphoric acid (Component B), Nitrite standard solution comprised of 1.0 mM sodium nitrite in deionized water (Component C). All components were kept in a 5 °C fridge, away from light.

PGE2 ELISA

Contents of Invitrogen PGE2 ELISA Kit (Thermo Fisher Scientific) - Antibody Coated 96-well plate, reagent diluent, PGE2 antibody, PGE2-AP (Alkaline phosphatase-conjugated PGE2), PGE2 standard (50 000 pg/ml), 20× wash buffer, substrate solution, and plate sealer.

Western Blot Analysis

Mini-PROTEAN TGX precast gels (Biorad) were utilised for loading samples and running electrophoresis within a Mini-PROTEAN Tetra System gel tank (Biorad) connected to PowerPac Basic (Biorad) power supply. A constant voltage was maintained throughout the run and the tank was kept in an ice-bath to maintain a cool system and prevent skewing of protein bands and dye front. Digital heat Block (Benchmark Scientific) was used to heat samples, Heidolph magnetic stirrer MR 2002 for mixing. A Mini-PROTEAN Gel releaser was used to pull apart and open cassette gel plates, ChemiDoc MP Imaging System (Biorad) for activating and visualising bands, and a roller for ironing out wrinkles and bubbles in the gel or membrane. Mini Trans-Blot Turbo 0.2 µm nitrocellulose Transfer pack (Biorad, USA) and Trans-Blot Turbo Transfer System (Biorad, Singapore) was utilised to transfer bands from the gel

onto membrane, and the E-OMM-A analogue orbital microplate mixer (Eins-Sci) for agitating. 500 µl Eppendorf tubes were used for mixing and storing protein samples, emptied pipette tip containers were repurposed for keeping the gel/membrane in working buffer or incubation solutions, forceps were used for moving membrane. Micropipettes, pasteur pipettes, beakers and measuring cylinders were used for preparing mixtures and transferring reagents.

2. Tables

Table A 1: IC10 values of the various treatments in LPS-stimulated RAW macrophages

Extract/ Drug	**IC10 (µg/ml)**
Hexane	12.5
Acetone	8.80
Methanol	undefined
E+H	23.0
SCF	10.2
MTX	1.00

3. Figures

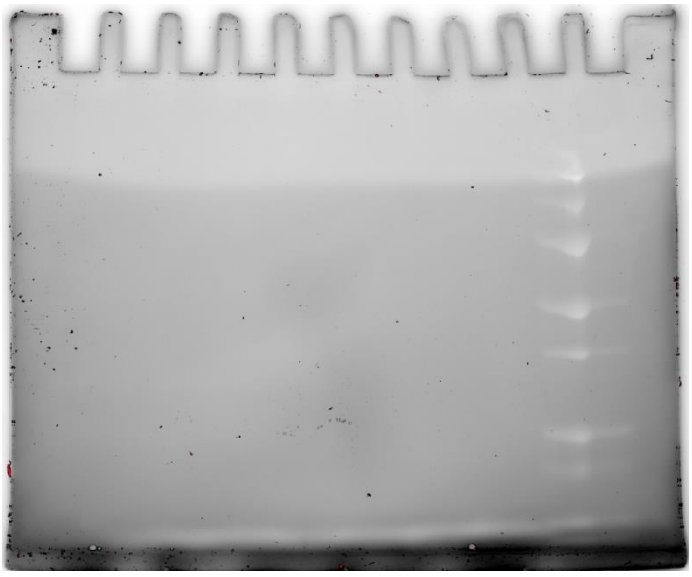

Figure A 1: Stain free gel image after electrophoresis. The bands on the right show

migration of the protein ladder.

NAFS
National · Analytical · Forensic · Services

Accredited by:
SAHPRA
South African Health Products Regulatory Authority

NAFS
109 Sovereign Drive
Route 21 Corporate Park
Centurion
0178

Certificate of Analysis

Sample ID:	230824-008-001
Retention Sample ID:	16,653
Client (Code) Name:	(CAN0525) Bushveld Genetics
Client Address:	Kameelhoek Farm, Farm 408, KQ portion 2, Limpopo, 0370
Batch:	Batch 0001 (Cannabis Crude Oil)
Date Receipt:	*8/28/2023 10:47:01AM*
Date Report Released:	*9/4/2023 10:56:40AM*
Sample Type:	Extract
Package Condition:	Intact
Received By:	AWRBKA
Sample Amount:	1 gram
Tamper Proof:	No

Test Name: **TM006.3 (Potency Cannabis HPLC) (230824-008-001)**
Specification: N/A
Test Method: *TM006.3
Sampling Method: SH007

Analyte	Results		*Std Dev.		*Spec Limits
CBC	ND	% Weight		% Weight	N/A
CBD	ND	% Weight		% Weight	N/A
CBD-A	ND	% Weight		% Weight	N/A
CBD-V	ND	% Weight		% Weight	N/A
CBG	ND	% Weight		% Weight	N/A
CBG-A	0.921	% Weight	+- 0.049	% Weight	N/A
CBN	ND	% Weight		% Weight	N/A
Delta-8-THC	ND	% Weight		% Weight	N/A
Delta-9-THC	12.036	% Weight	+- 0.393	% Weight	N/A
THC-A	36.474	% Weight	+- 0.578	% Weight	N/A
THC-V	ND	% Weight		% Weight	N/A
Total Potential CBD	ND	% Weight		% Weight	N/A
Total Potential THC	44.024	% Weight	+- 0.900	% Weight	N/A

Analyst: *ANAIDOO* 2023/08/31 15:27

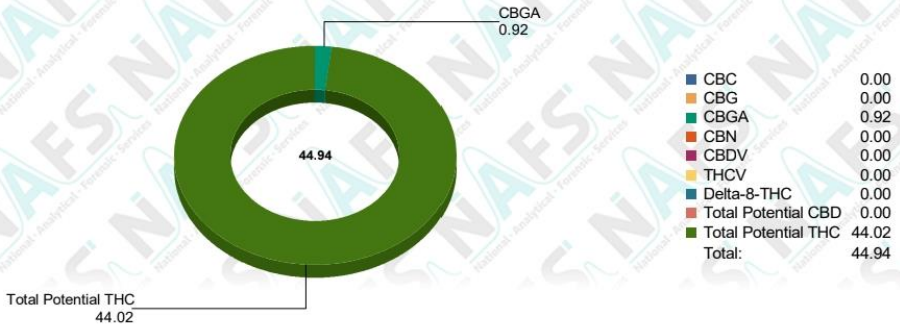

National · Analytical · Forensic · Services

Report Generated: 9/4/2023 10:56:50AM

Email: info@NAFS.co.za
Tel: 087 654 6237

NAFS
National · Analytical · Forensic · Services

Accredited by:
SAHPRA
South African Health Products Regulatory Authority

NAFS
109 Sovereign Drive
Route 21 Corporate Park
Centurion
0178

Test Name: **TM003.5 (Terpenes) (230824-008-001)**
Specification: N/A
Test Method: *TM003.5
Sampling Method: SH007

Analyte	Results		*Std Dev.		*Spec Limits
Alpha-Bisabolol	3.232	mg/g	+- 0.231	mg/g	N/A
Alpha-Humulene	3.599	mg/g	+- 0.242	mg/g	N/A
Alpha-Pinene	1.682	mg/g	+- 0.129	mg/g	N/A
Alpha-Terpinene	ND	mg/g		mg/g	N/A
Beta-Caryophyllene	7.443	mg/g	+- 0.535	mg/g	N/A
Beta-Myrcene	3.156	mg/g	+- 0.276	mg/g	N/A
Beta-Pinene	0.869	mg/g	+- 0.053	mg/g	N/A
Camphene	ND	mg/g		mg/g	N/A
cis-Nerolidol	ND	mg/g		mg/g	N/A
Delta-3-Carene	ND	mg/g		mg/g	N/A
Gamma-Terpinene	ND	mg/g		mg/g	N/A
Geraniol	ND	mg/g		mg/g	N/A
Guaiol	1.297	mg/g	+- 0.128	mg/g	N/A
Isopulegol	ND	mg/g		mg/g	N/A
Limonene	1.542	mg/g	+- 0.112	mg/g	N/A
Linalool	1.090	mg/g	+- 0.055	mg/g	N/A
Ocimene	ND	mg/g		mg/g	N/A
Para-Cymene	ND	mg/g		mg/g	N/A
Terpinolene	ND	mg/g		mg/g	N/A
Total Nerolidol	0.832	mg/g	+- 0.032	mg/g	N/A
trans-Nerolidol	0.832	mg/g	+- 0.032	mg/g	N/A

Analyst: *ENAUDE* 2023/09/04 10:44

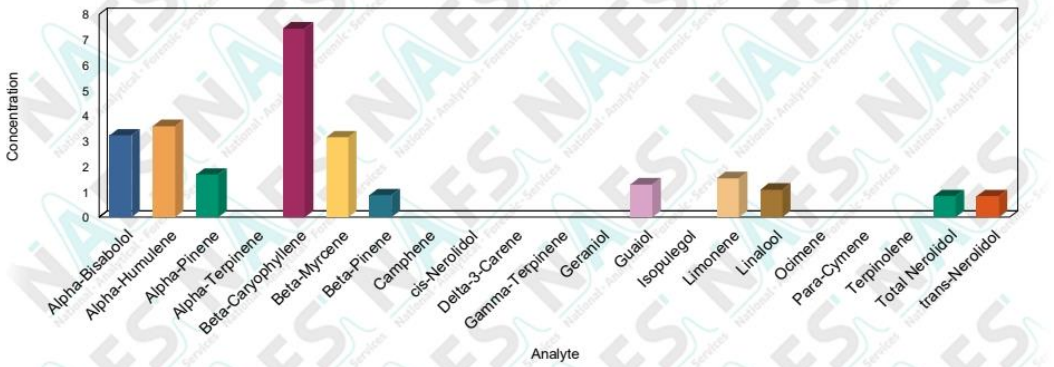

*ND (Not Detected)
*The current test method version is Validated
*Standard Deviation (Uncertainty of measurement of applicable duplicate sample)
*Specificaiton Limits (Specified according to pharmacopeial or client specification limits where applicable)

National · Analytical · Forensic · Services

Accredited by: SAHPRA South African Health Products Regulatory Authority

NAFS
109 Sovereign Drive
Route 21 Corporate Park
Centurion
0178

Interpretations and Opinions:

There was matrix interference detected within the retention windows of alpha-Bisabolol and Guaiol. This could result in the reported values being either higher or lower than the actual result.

Additions, Deviations & Exclusions:

None

It should be noted that NAFS will only analyze the sample/s received. This sample cannot be regarded as representative of entire batch or crop. It is the responsibility of the client to ensure a representative sample is taken in an appropriate tamper proof sample container. NAFS cannot be held liable for negligent handling, storage and transport of client samples, prior to receipt. Any complaints may be directed toward NAFS using info@nafs.co.za (QA005)

Quality Assurance Manager

Released By: *Lindie Marais*

Released On: *9/4/2023 10:56:40AM*

Figure A 2: Certificate of analysis of SCF extract

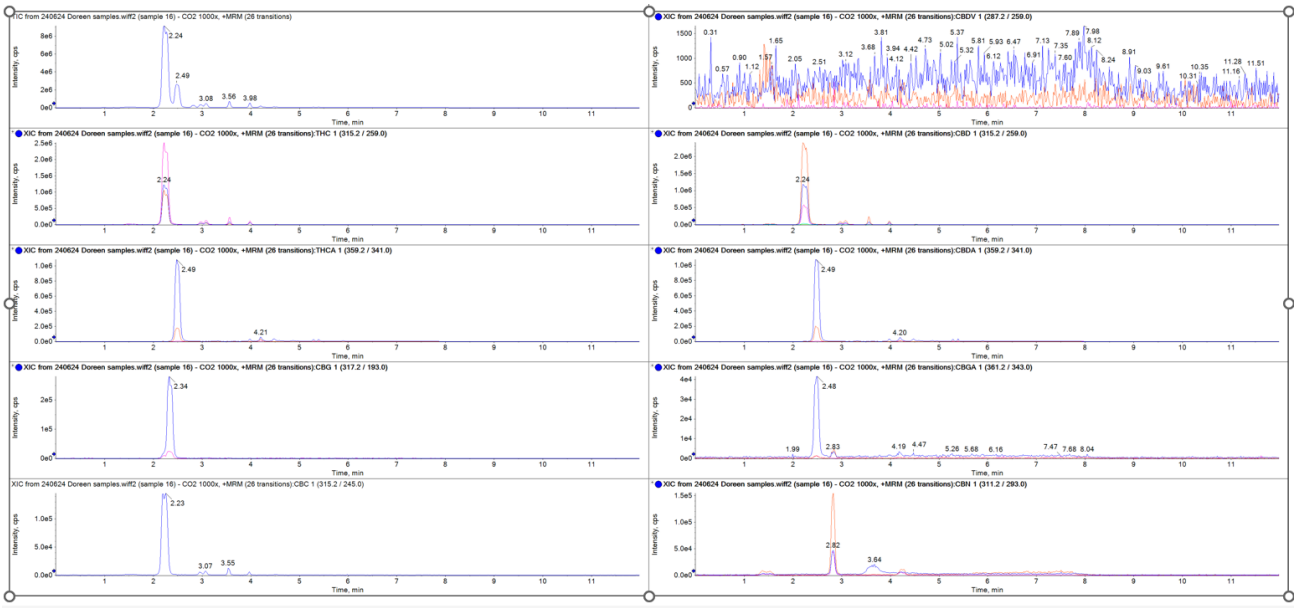

Figure A 3: SCF extract LC-MS chromatograms. CO_2=SCF

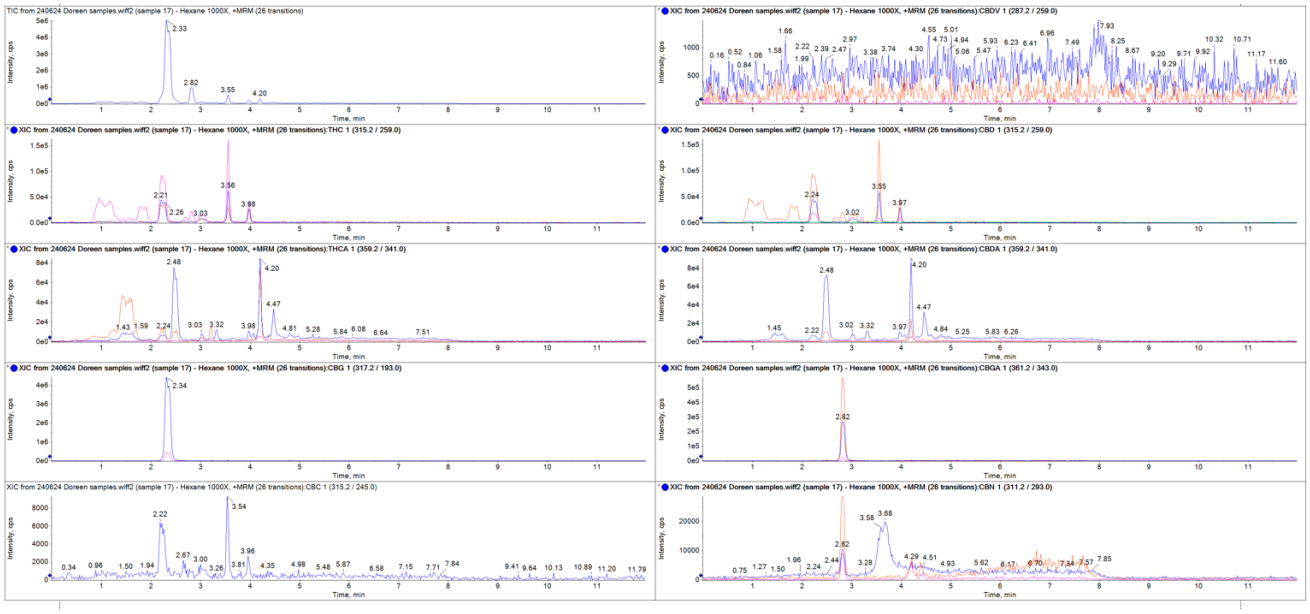

Figure A 4: Hexane extract LC-MS chromatograms.

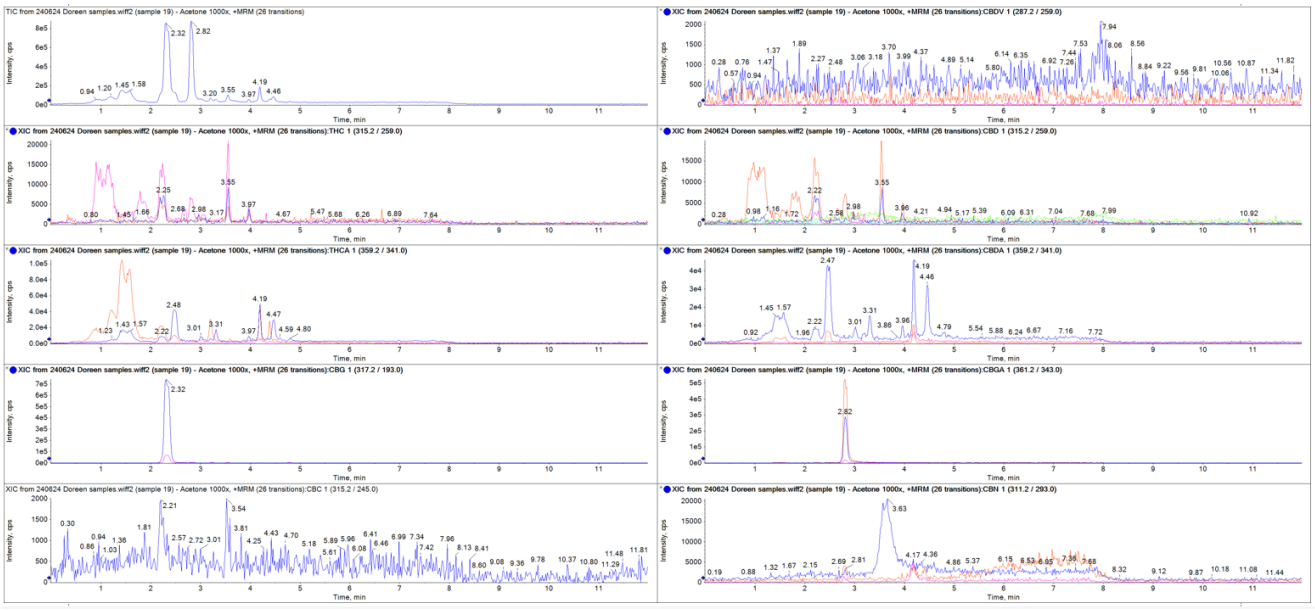

Figure A 5: Acetone extract LC-MS chromatograms.

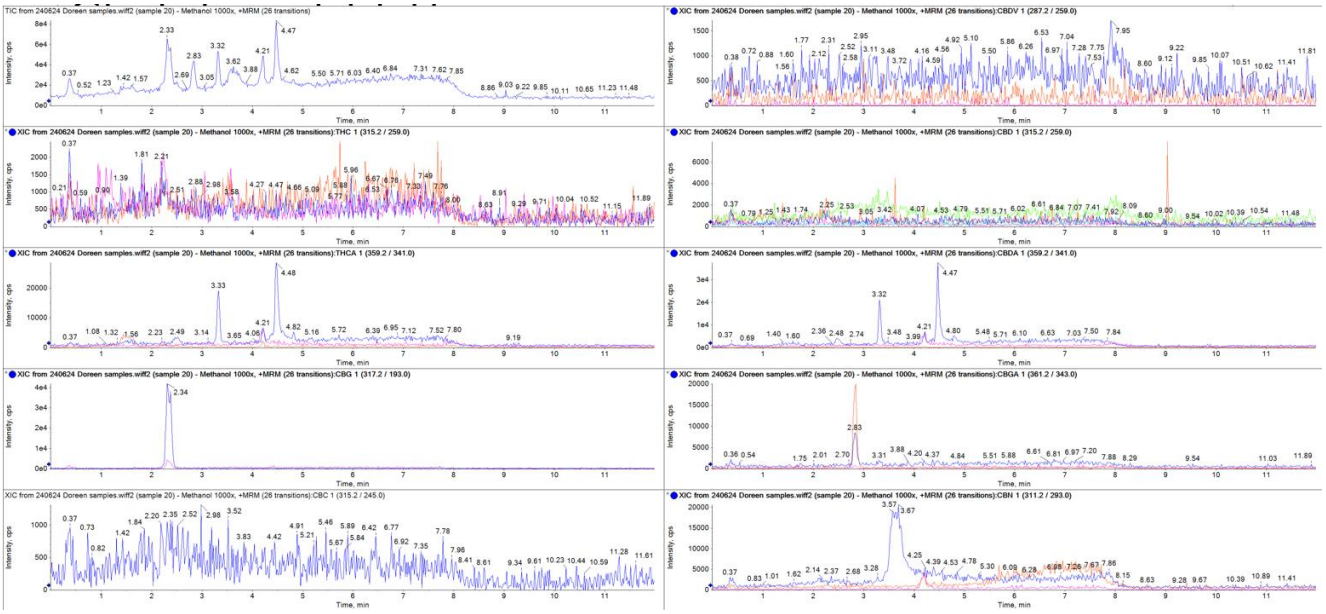

Figure A 6: Methanol extract LC-MS chromatograms.

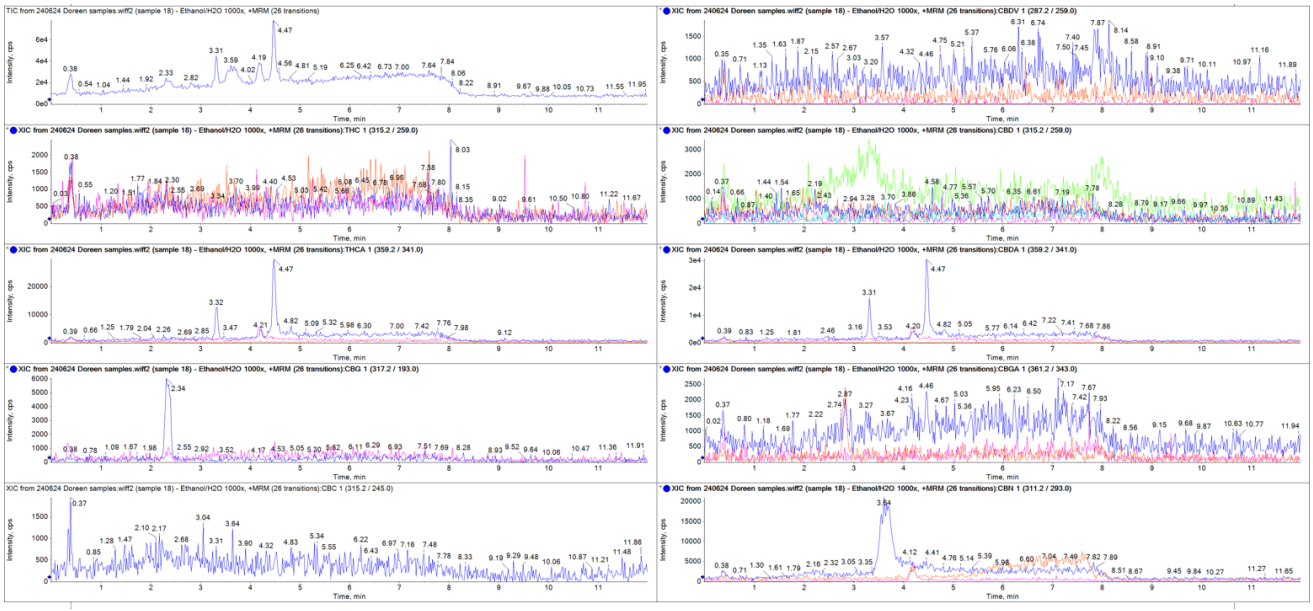

Figure A 7: E+H extract LC-MS chromatograms.

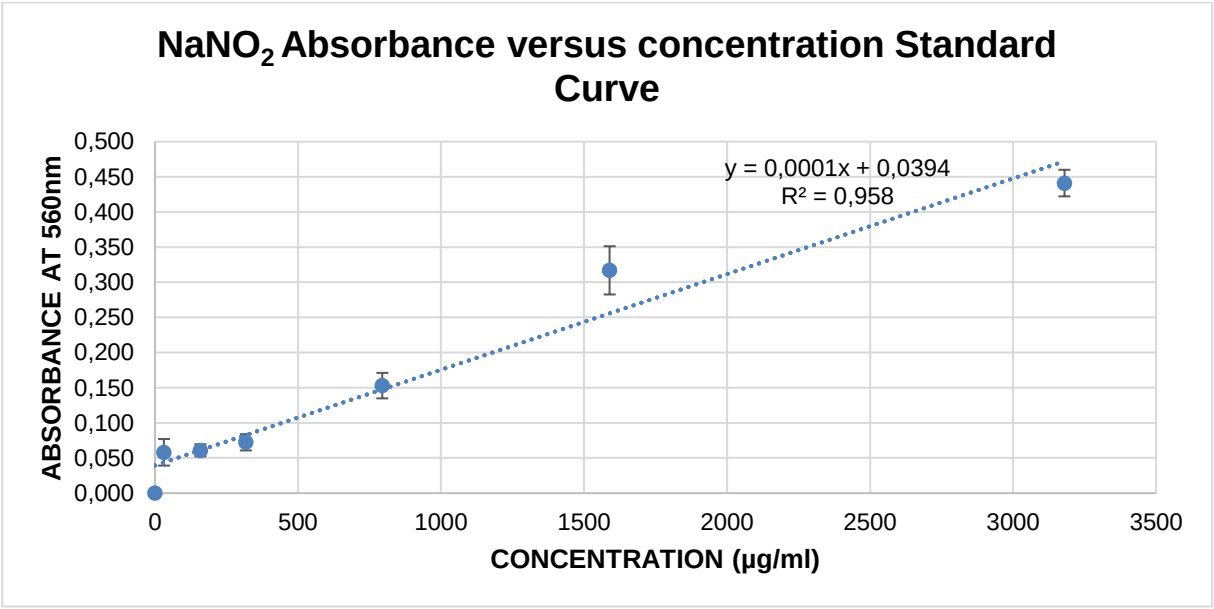

Figure A 8: Standard absorbance graph of $NaNO_2$ at various known concentrations.

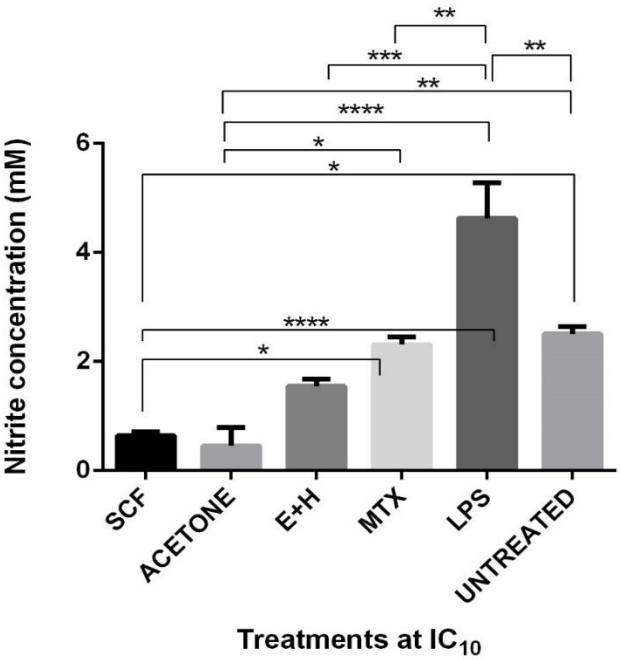

Figure A 9: Nitrite concentrations in treated, LPS-stimulated and untreated RAW 264.7 macrophages. Statistically significant differences between treatment groups are also shown above.

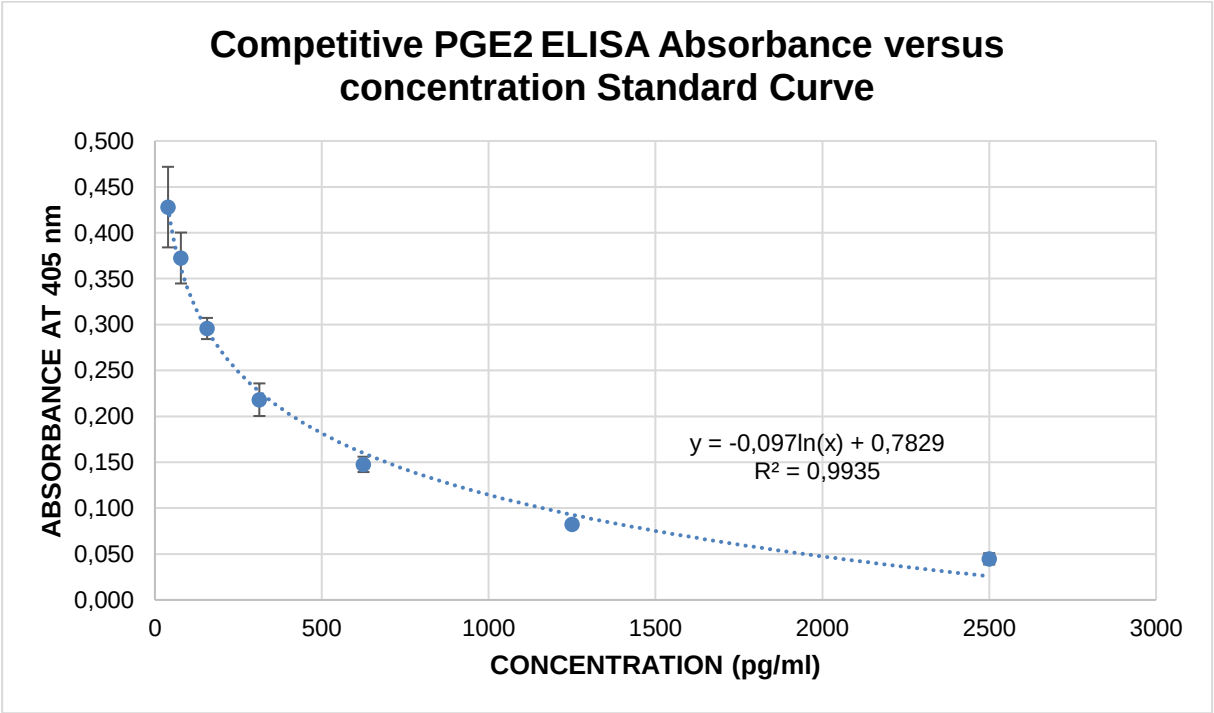

Figure A 10: Standard absorbance graph of PGE2 at various known concentrations.

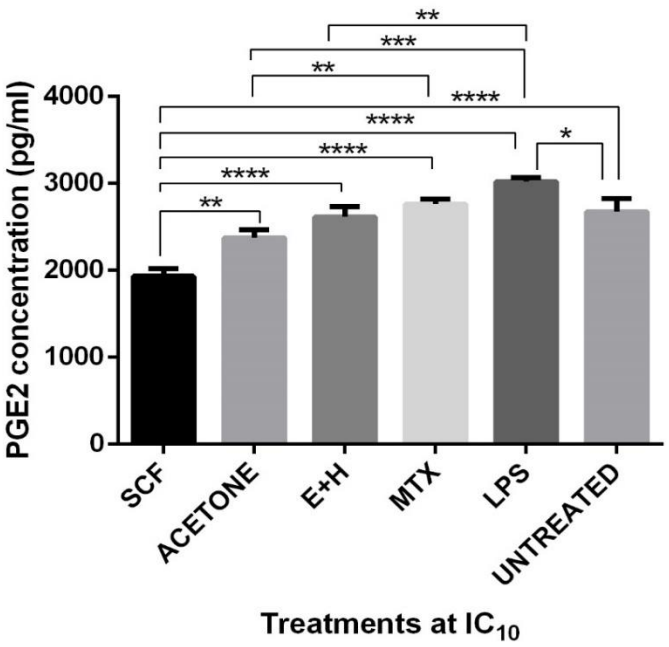

Figure A 11: PGE2 concentrations in treated, LPS-stimulated and untreated RAW 264.7 macrophages. Statistically significant differences between treatment groups are also shown above.

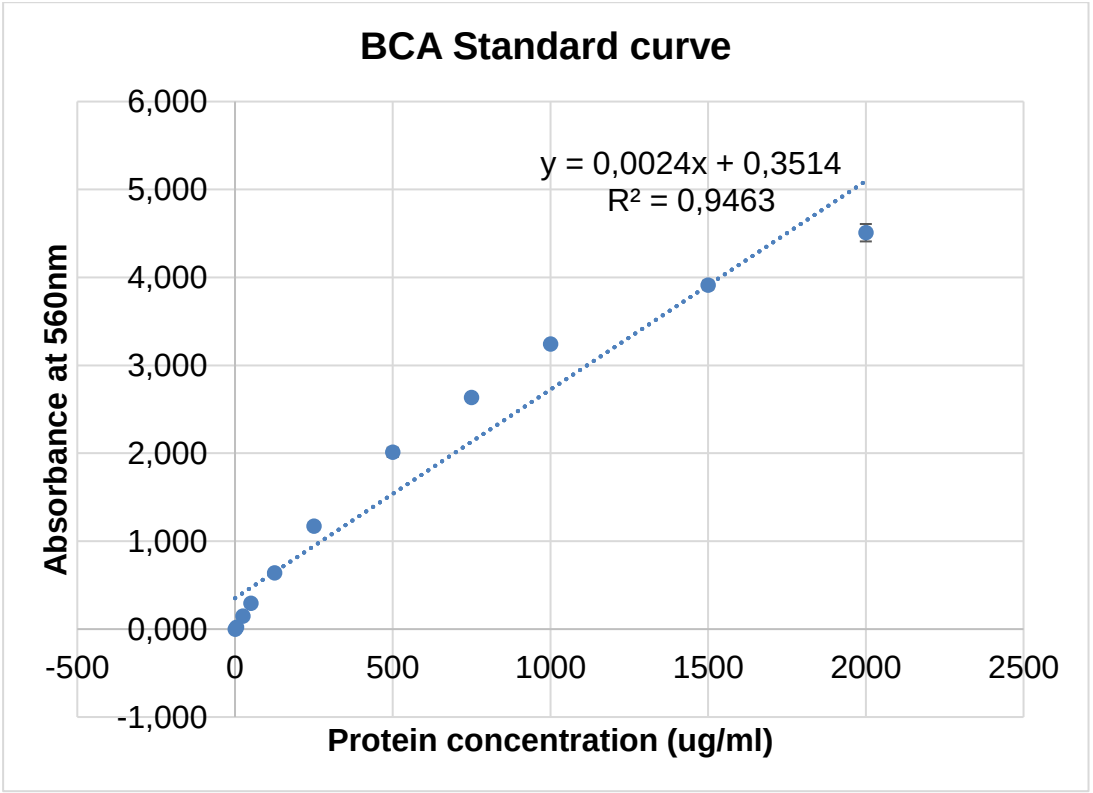

Figure A 12: Standard absorbance graph of BSA protein at various known concentrations.

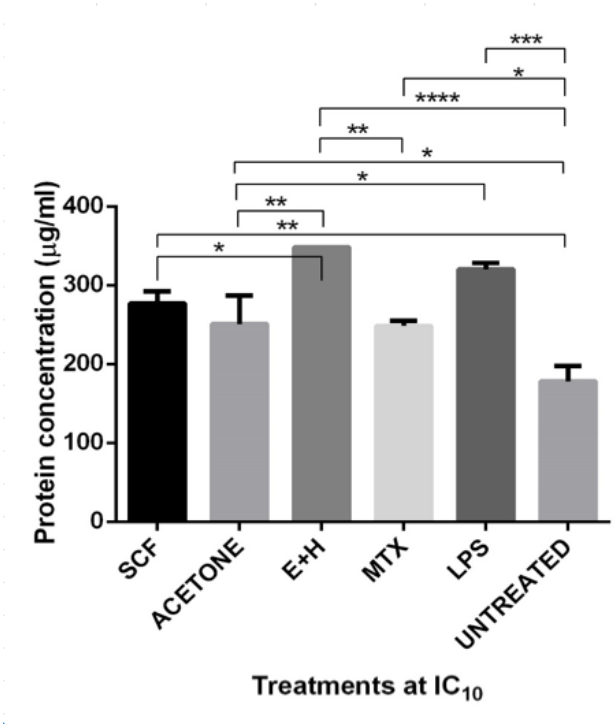

Figure A 13: Protein concentrations in treated, LPS-stimulated and untreated RAW 264.7 macrophages. Statistically significant differences between treatment groups are also shown above.